THE APPLICATION OF HOLOGRAPHIC INTERFEROMETRY TO THE DETERMINATION OF DISCONTINUOUS THREE-DIMENSIONAL DENSITY FIELDS

Paul Edgar Van Houten

NAVAL POSTGRADUATE SCHOOL
Monterey, California

THESIS

THE APPLICATION OF HOLOGRAPHIC INTERFEROMETRY
TO THE DETERMINATION OF
DISCONTINUOUS THREE-DIMENSIONAL DENSITY FIELDS

by

Paul Edgar Van Houten

Thesis Advisor: D.J. Collins

December 1972

The Application of Holographic Interferometry to the Determination of Discontinuous Three-Dimensional Density Fields

by

Paul Edgar Van Houten
Lieutenant, United States Navy
B.S., University of Mississippi, 1965

Submitted in partial fulfillment of the
requirements for the degree of

AERONAUTICAL ENGINEER

from the

NAVAL POSTGRADUATE SCHOOL
December 1972

ABSTRACT

A fourier transform method is used to invert the integral equation resulting from holographic interferometry of three-dimensional weakly refractive phase objects. The inverted equation is applied to the determination of aerodynamic density fields. The effects of various numerical techniques are extensively evaluated in an attempt to minimize computational effort. Numerical filtering techniques are introduced in order to handle the discontinuities associated with supersonic aerodynamic phenomenon.

TABLE OF CONTENTS

I. INTRODUCTION ---------- 7

II. HOLOGRAPHIC INTERFEROMETRY ---------- 9

III. FRINGE INTERPRETATION ---------- 13

A. LIVE FRINGE ---------- 13

B. FROZEN FRINGE ---------- 13

C. INFINITE FRINGE ---------- 13

D. FINITE FRINGE ---------- 13

IV. FOURIER TRANSFORMS ---------- 15

V. INTEGRAL INVERSION ---------- 17

A. THE INTEGRAL EQUATION ---------- 17

B. THE FOURIER INTEGRAL SOLUTION ---------- 19

VI. NUMERICAL METHOD ---------- 24

A. PROGRAM PARAMETERS ---------- 24

B. THE INFINITE ρ INTEGRATION ---------- 25

C. THE INTEGRATION OVER PHI ---------- 27

VII. PROGRAM TESTING ---------- 29

A. TEST INVERSIONS ---------- 29

1. Axisymmetric Gaussian ---------- 29

2. Axisymmetric Shock ---------- 29

3. Axisymmetric Shock With Restricted Data - 30

4. Asymmetric Gaussian ---------- 30

B. INVERSIONS OF ACTUAL DATA ---------- 30

VIII. DISCUSSION OF RESULTS ---------- 32

A. TEST INVERSIONS ---------- 32

1. Axisymmetric Gaussian Inversion --------- 32
2. Axisymmetric Step Function ---------- 33
3. Restricted Radial Coverage ---------- 34
4. Asymmetric Test Case ---------- 35
B. INVERSION OF ACTUAL DATA ---------- 35
1. Axisymmetric Free-jet ---------- 35
2. Asymmetric Free-jet ---------- 36
IX. CONCLUSIONS AND RECOMMENDATIONS ---------- 38
FIGURES ---------- 39
COMPUTER PROGRAM ---------- 49
LIST OF REFERENCES ---------- 66
INITIAL DISTRIBUTION LIST ---------- 67
FORM DD 1473 ---------- 68

LIST OF FIGURES

1. Production of a Hologram of a Transilluminated Object ---------- 39
2. Hologram of a Diffusely Reflecting Object -------- 39
3. Basic Coordinates of the Inversion ---------- 40
4. Axisymmetric Gaussian ---------- 41
5. Axisymmetric Shock ---------- 41
6. Axisymmetric Double Shock ---------- 42
7. Incomplete Fringe Coverage ---------- 42
8. Asymmetric Test Case ---------- 43
9. Axisymmetric Free-jet Z = .05 cm ---------- 44
10. Axisymmetric Free-jet Z = .5 cm ---------- 44
11. Tiled, 60 PSIG Free-jet ---------- 45
12. Typical Variation of Integrand ---------- 46
13. Fringe Shift and Value of the Inside Integral From the Axisymmetric Shock ---------- 46
14. Fringe Data of a Phase Object with One Degree of Symmetry ---------- 47
15. $G(\rho_L,\phi_k)$ For Points (x_o,y_o) From An Axisymmetric Step Function ---------- 48

ACKNOWLEDGEMENT

The author would like to express his gratitude to Professor D. J. Collins for his valuable assistance and guidance during the investigation, to Mr. Norman E. Leckenby for his logistic support during the time it became necessary to play musical buildings with our holographic equipment, and to my wife for her assistance with the clerical chores associated with the production of the thesis.

I. INTRODUCTION

Holographic interferometry offers a means of determining three-dimensional density fields created by aerodynamic phenomenon. Pulsed lasers, with good spatial and temporal coherence with double-exposed holograms have eliminated the need for high quality optical components. The short pulse of the giant-pulse lasers allows the aerodynamicist to "freeze" transient phenomenon in the interferometric views around the test section.

Interferometric data is obtained by superimposing a hologram of the test section without flow and a hologram of the test section with flow. The superposition is accomplished by double exposure of the same holographic plate. When the double-exposed hologram is viewed, phase differences in the two views result in light and dark regions. By counting the number of light and dark regions in going from an undisturbed region to the point of interest, one obtains the fringe number for that point. The phase difference is determined by the total difference in optical path length, resulting from the aerodynamic phenomenon. The relative refractive index [f(x,y)] is a function of the density [$\rho(x,y)$].

$$f(x,y) = \frac{\beta}{\rho_s \lambda} \left(\frac{\rho(x,y)}{\rho_\infty} - 1\right) \qquad \text{Eq. (1)}$$

where ρ_s is the density of the gas at which β is measured.

To determine the refractive index from the fringe data available around the test section $g(\rho,\theta)$, one must invert the integral equation.

$$g(\rho,\theta) = \int_{L_1}^{L_2} f(x,y)\, dv$$

By utilizing a two-dimensional fourier transform method [Ref. 4], it has been shown that the refractive index at a point (X_o,Y_o) in the test section can be expressed as

$$f(X_o,Y_o) = \frac{1}{2\pi^2} \int_{-\frac{\pi}{2}}^{+\frac{\pi}{2}} \int_{0}^{\infty} \frac{g(\rho_0+\rho,\theta)+g(\rho_o-\rho,\theta)-2g(\rho_o,\theta)}{\rho^2} d\rho d\theta$$

The fourier transform method requires less computational effort than the previously utilized methods of

1. Fourier expansion of the unknown function $f(x,y)$ in appropriate orthogonal polynomials. [Ref. 1]

2. Representing the unknown functions by discrete cubes and solving the resulting set of simultaneous linear equations.

The computerized method developed yields results which compare favorably with the fourier expansion method of Matulka [Ref. 1]. The computation time was reduced by a factor greater than twenty. Errors resulting from the fourier transform method were greater than those associated with the fourier expansion method of Reference 1. The reduced computation time more than offsets the slightly larger errors associated with the fourier transform method.

II. HOLOGRAPHIC INTERFEROMETRY

The ability of a hologram to record both amplitude and phase variations has greatly extended the capabilities of interferometric analysis. When a hologram storing more than one wave pattern is illuminated with coherent light, the reconstructed waves interfere with each other, producing fringe patterns which yield quantitative information concerning the disturbance causing the interference. Since the two wavefronts were constructed utilizing the same optical paths, the optical components are automatically matched and only the changes in the subject create the visible fringe patterns.

The effective reconstruction of the wavefront by holography requires that the coherent light of a laser be separated into two beams (Fig. 1), the object or scene beam which illuminates the subject (modulated), and the reference beam which is reflected from an optically flat mirror (unmodulated). The path-lengths of the two beams must be approximately equal due to the finite coherency length of available lasers (10 cm - 1 m).

In order to simplify the development of the reconstruction process, assume the reference beam is collimated, although this is not necessary in practice. Since the exposure time of the film represents a time average of the intensity, the temporal portion of the wavefronts, $e^{j\omega t}$ may be neglected

and only spatial variations in the plane of the photographic plate considered. Let $U_o(x,y)$ denote the complex amplitude of the reference beam. Since this beam is plane

$$U_o(x,y) = a_o\, e^{i(\alpha x + \beta y)}$$

where α and β are the spatial frequencies of the reference beam in the x,y plane of the holographic plate (cycles/mm).

Similarly let $U(x,y)$ denote the complex amplitude of the scene beam

$$U(x,y) = a(x,y)\, e^{i(\phi(x,y))}$$

The intensity $I(x,y)$ thus recorded by the photographic film is given by the expression

$$I(x,y) = |U+U_o|^2 = a^2+a_o{}^2+aa_o e^{i[\phi(x,y)-\alpha x-\beta y]}$$

$$+aa_o e^{-i[\phi(x,y)-\alpha x-\beta y]}$$

$$= a^2+a_o{}^2+2aa_o \cos[\phi(x,y)-\alpha x-\beta y]$$

When the exposed hologram is developed, the transmittance will be proportional to the intensity $I(x,y)$. Illumination of the hologram by a plane beam $U_r(x,y)$ similar to the reference beam yields a transmitted beam $U_t(x,y)$ given by

$$U_t(x,y) = U_r(x,y)[1-kI(x,y)]$$

$$= [1-k(a^2+a_o^2)]U_r(x,y)-a_o^2kU(x,y)-ka(x,y)U_r^{*2}$$

where k is the constant of proportionality of the photographic emulsion.

The illuminating beam produces a direct beam and two first-order diffracted beams on either side of the direct beam. The term $ka_o^2U(x,y)$ represents the diffracted beam that produces the virtual image. The last term produces the real image with inverted depth. The negative sign for the two diffracted beams simply represents a 180 degree phase shift to which the eye is insensitive.

If we consider only the virtual image formed by double exposure to two complex wavefronts, the transmitted virtual image is given as

$$U_t(x,y) = -k[a_o^2(a_1(x,y)e^{i\phi_1(x,y)}+a_2(x,y)e^{i\phi_2(x,y)})]$$

Hence illumination of the double-exposed hologram not only effects the simultaneous reconstruction of the two waves but causes them to interfere.

Although it is not necessary for the original reference beam to be collimated, if the re-illumination beam is different from the reference beam, the reconstructed diffraction beams are distorted accordingly. Since a

collimated beam is the easiest to duplicate, a collimated reference beam should be used when possible.

For a more detailed and complete analysis of holography, Reference 2 is recommended.

III. FRINGE INTERPRETATION

By utilizing different methods of superimposing the two wavefronts, various fringe patterns may be observed.

A. LIVE FRINGE

Live fringe patterns are generated when the hologram is exposed, developed, replaced exactly in its original position, and re-illuminated. The stored wavefront in the hologram interferes with the "live" wavefront from the subject. This technique requires precise repositioning of the hologram plate and readjustment of the scene beam's intensity.

B. FROZEN FRINGE

Frozen fringe patterns are produced by the double exposure of the hologram prior to development. The double-exposed hologram need not be restored to its original position in order to view the fringe patterns. Illumination by a beam similar to the original reference beam is quite adequate.

C. INFINITE FRINGE

Infinite fringe patterns are seen if the two wavefronts viewed through the hologram utilized the exact same optical arrangement for construction. The visible fringe patterns are focused at infinity.

D. FINITE FRINGE

Finite fringe patterns occur when finite displacements are introduced in the optical arrangement between exposures

of the hologram plate. The displacements usually used are small rotations of one of the mirrors in either the reference or scene beams, translation of the diffusely illuminating screen, or translation of the diffusely illuminating screen, or translation of the hologram plate [Ref. 3]. If there is no disturbance of the subject between exposures, these small translations ($d = r\theta \simeq .003$ inches) result in parallel interference lines which are perpendicular to the direction of translation. The parallel lines form a convenient scale for determining fringe orders. The fringe pattern will be focused somewhere within the phase object [Ref. 3].

In conventional holography, three-dimensionality is accomplished by recording the wavefront created by the diffusely reflected light from the subject [Fig. 2]. Each point on the subject is a point light source which interferes with all other point light sources on the subject. This same three-dimensionality may be retained in holograms of transparent objects by placing a diffuser plate in the scene beam prior to the test section [Fig. 1]. The localization of fringe patterns is greatly enhanced by using these "light-field" interferograms.

The utilization of frozen, finite fringe patterns on lightfield interferograms yields good results when dealing with aerodynamic phenomenon associated with wind tunnel experiments.

IV. FOURIER TRANSFORMS

With appropriate restrictions [Ref. 2], optical systems may be considered linear, space invariant systems. As linear space invariant systems, they may be analyzed using Fourier-transform techniques. Temporally modulated waves may be analyzed in either of two domains; a temporal domain or a temporal frequency domain. Analogously, spatially modulated waves may be analyzed in either a spatial domain or a spatial frequency domain.

In the spatial domain, the light complex amplitude $a(x,y)$ is expressed as a function of the (x,y) spatial coordinates. The same complex amplitude can be expressed in terms of orthogonal spatial frequencies α and β (rads/mm) as well. Thus the light's complex amplitude distribution $a(x,y)$ in the spatial domain may be expressed as another function $A(\alpha,\beta)$ in the spatial frequency domain. The two functions are related through the two-dimensional transform pair

$$A(\alpha,\beta) = \frac{1}{\sqrt{2\pi}} \int_{-\infty}^{\infty} \int_{-\infty}^{\infty} a(x,y)\, e^{i(\alpha x + \beta y)}\, dx\, dy$$

and

$$a(x,y) = \frac{1}{\sqrt{2\pi}} \int_{-\infty}^{\infty} \int_{-\infty}^{\infty} A(\alpha,\beta)\, e^{-i(\alpha x + \beta y)}\, d\alpha\, d\beta$$

To every function in the spatial domain, there usually is a corresponding function in the spatial frequency domain. Similarly for every operation in the spatial domain, there is a corresponding operation in the spatial frequency domain. The advantage of Fourier analysis is that the operation in the spatial frequency domain may be much easier than the corresponding operation in the spatial domain. The multiplier $(1/\sqrt{2\pi})$ is used since most Fourier transform tables list the transform pairs such that the total multiple is $\frac{1}{2}\pi$.

V. THE INTEGRAL INVERSION

A. THE INTEGRAL EQUATION

The information available from the hologram [Fig. 3] is in the form of fringe numbers. The relative phase delay experienced by straight line rays passing through the phase object determines the fringe number at some point of the hologram.

If $n(x,y,z)$ is the index of refraction with the phase object present, and $n_o(x,y,z)$ is the index of refraction without the phase object, the relative phase in wavelengths is

$$g(\rho,\theta,z) = \int_{L_1}^{L_2} \left[\frac{n(x,y,z) - n_o(x,y,z)}{\lambda}\right] d\nu \qquad (1A)$$

where $(L_2 - L_1)$ is the total distance of travel of each parallel ray through the phase object. From Figure 3 the relationship of the coordinates (ρ,ν) to (x,y) for a given ray direction (θ) is

$$x = \nu \sin\theta + \rho \cos\theta \qquad (2A)$$

$$y = -\nu \cos\theta + \rho \sin\theta \qquad (2B)$$

The refractive index of gas as a function of density is given by the first two terms of the Taylor expansion (Liepmann and Rushko,1957).

$$n = 1 + \beta \rho/\rho_s$$

where ρ_s is the density of the gas at which β is measured. For air at zero degrees centigrade and 760 mm Hg

$$\rho_s = .0012929 \text{ gm/cc}$$

$$\beta = .00291 \quad \text{for deep red light}$$

Hence:

$$\rho(x,y,z) = \rho_o(x,y,z) + \frac{\rho_s \lambda}{\beta} \left[\frac{n(x,y,z) - n_o(x,y,z)}{\lambda}\right] \tag{3}$$

The wavelength (λ) is maintained because of the form of Eq. (1A)

$$\text{Let} \quad f(x,y,z) = \frac{n(x,y,z) - n_o(x,y,z)}{\lambda}$$

By choosing the (x,y) plane parallel to the rays, the z coordinate becomes a parameter and Eq. (1) can be written

$$g_z(\rho,\theta) = \int_{L_1}^{L_2} f_z(x,y)\, d\nu \tag{1B}$$

The parameter z will be dropped from further discussion.

Previous solutions to the three-dimensional refractive index problem utilized Fourier series techniques [Ref. 1] and required excessive calculations. The method proposed by

Rowley [4], as modified by Junginger and Haeringen [5], offers good results for a minimum of calculations.

B. THE FOURIER INTEGRAL SOLUTION

The limits of Equation 1A can be extended to infinity because f(x,y) is zero outside the phase object.

$$g(\rho,\theta) = \int_{-\infty}^{\infty} f(x,y)\, d\nu \qquad (1C)$$

The function f(x,y) may be described by the Fourier integral.

$$f(x,y) = \frac{1}{\sqrt{2\pi}} \int_{-\infty}^{\infty}\int_{-\infty}^{\infty} F(\alpha,\beta)\, e^{-i(\alpha x + \beta y)}\, d\alpha\, d\beta \qquad (4A)$$

Substituting equations (2A), (2B), and (4A) into (1C) and integrating first on ν gives

$$g(\rho,\theta) = \frac{1}{\sqrt{2\pi}} \int_{-\infty}^{\infty}\int_{-\infty}^{\infty} F(\alpha,\beta)\, e^{-i\rho(\alpha\cos\theta+\beta\sin\theta)}\, d\alpha\, d\beta$$

$$\int_{-\infty}^{\infty} e^{i\nu(\alpha\sin\theta-\beta\cos\theta)}\, d\nu \qquad (5)$$

The Dirac-Delta function has the following transform.

$$\delta(t_o-t) = \frac{1}{2\pi} \int_{-\infty}^{\infty} e^{i\omega(t_o-t)}\, d\omega \qquad (6)$$

Hence the last integral of equation (5) is simply

$$\int_{-\infty}^{\infty} e^{i\nu(\alpha\sin\theta-\beta\cos\theta)} d\nu = 2\pi\delta(\alpha\sin\theta-\beta\cos\theta)$$

$$= \frac{2\pi}{|\cos\theta|}\, \delta(\alpha\tan\theta-\beta)$$

Because of the properties of the delta function, if we now integrate over β, Equation (5) reduces to

$$g(\rho,\theta) = \sqrt{2\pi} \int_{-\infty}^{\infty} F(\alpha,\beta=\alpha\tan\theta)\, e^{-i\rho\frac{\alpha}{\cos\theta}} \frac{d\alpha}{|\cos\theta|} \quad (7)$$

Equation (7) has the Fourier inverse

$$F(\alpha,\beta=\alpha\tan\theta) = \frac{1}{(2\pi)^{3/2}} \int_{-\infty}^{\infty} g(\rho,\theta) e^{i\rho\frac{\alpha}{|\cos\theta|}}\, d\rho \quad (8)$$

Although Equation (8) and (4A) may be used to determine the refractive index, there are numerical difficulties associated with the infinite integrals of Equation (4A). The problem can be further simplified as suggested by Junginger and Haeringer [5].

For a given point (x_o,y_o), substitution of Equation (8) into Equation (4A) gives

$$f(x_o,y_o) = \frac{1}{4\pi^2} \int_{-\infty}^{\infty}\int_{-\infty}^{\infty}\int_{-\infty}^{\infty} g(\rho,\theta) e^{\left(i\frac{\rho\alpha}{|\cos\theta|}-\alpha x_o-\beta y_o\right)} d\rho d\alpha d\beta \quad (4B)$$

Introducing polar coordinates in the Fourier frequency domain

$$\theta = \arctan \beta/\alpha$$

$$k = (\alpha^2 + \beta^2)^{1/2} = \frac{\alpha}{|\cos\theta|}$$

From Figure (3)

$$\rho_o = x_o \cos\theta + y_o \sin\theta$$

Equation (4B) becomes

$$f(x_o,y_o) = \frac{1}{4\pi^2} \int_0^{2\pi} \int_0^{\infty} \int_{-\infty}^{\infty} g(\rho,\theta) e^{\left(i\rho\frac{\alpha}{|\cos\theta|} - \rho_o\frac{\alpha}{\cos\theta}\right)} d\rho k dK d\theta$$

Separating the integral over theta yields

$$f(x_o,y_o) = \frac{1}{4\pi^2} \int_{-\frac{\pi}{2}}^{\frac{\pi}{2}} \int_0^{\infty} \int_{-\infty}^{\infty} g(\rho,\theta)\, e^{ik(\rho-\rho_o)} d\rho\, k dk\, d\theta$$

$$+ \frac{1}{4\pi^2} \int_{\frac{\pi}{2}}^{\frac{3\pi}{2}} \int_0^{\infty} \int_{-\infty}^{\infty} g(\rho,\theta)\, e^{ik(\rho+\rho_o)}\, d\rho\, k dk\, d\theta$$

Utilizing the fact that $g(-\rho,\theta)$ equals $g(\rho,\theta+\pi)$, the last term may be written as

$$+ \frac{1}{4\pi^2} \int_{-\frac{\pi}{2}}^{\frac{\pi}{2}} \int_0^{\infty} \int_{-\infty}^{\infty} g(\rho,\theta)\, e^{-ik(\rho-\rho_o)}\, d\rho\, k dk\, d\theta$$

Recombining the two terms yields

$$f(x_o,y_o) = \frac{1}{2\pi^2} \int_{-\frac{\pi}{2}}^{\frac{\pi}{2}} \int_0^{\infty} \int_{-\infty}^{\infty} g(\rho,\theta)\cos k(\rho-\rho_o)\, d\rho\, k dk\, d\theta \qquad (4C)$$

Performing the ρ integration by parts yields

$$f(x_o,y_o) = -\frac{1}{2\pi^2}\int_{-\frac{\pi}{2}}^{\frac{\pi}{2}}\int_{0}^{\infty}\int_{-\infty}^{\infty}\frac{\partial g(\rho,\theta)}{\partial\rho}\,\mathrm{sink}(\rho-\rho_o)\,d\rho\,dk\,d\theta \tag{9}$$

since $g(\pm\infty,\theta) = 0$.

The integrations over k and ρ can now be interchanged and the k integration can be evaluated. Equation (9) becomes

$$f(x_o,y_o) = -\frac{1}{2\pi^2}\int_{-\frac{\pi}{2}}^{\frac{\pi}{2}}\mathcal{P}\int_{-\infty}^{\infty}\frac{\partial g(\rho,\theta)}{\partial\rho}\,\frac{d\rho}{\rho-\rho_o}\,d\theta$$

where $\mathcal{P}$ stands for the principal value of the following integral. Using the definitions of the principal value and taking

$$\frac{\partial g(\rho,\theta)}{\partial\rho} = \frac{\partial[g(\rho,\theta)-g(\rho_o,\theta)]}{\partial\rho}$$

we find integrating by parts over ρ

$$f(x_o,y_o) = -\frac{1}{2\pi^2}\int_{-\frac{\pi}{2}}^{\frac{\pi}{2}}\int_{-\infty}^{\infty}[g(\rho_o+\rho,\theta)-g(\rho_o,\theta)]\frac{d\rho}{\rho^2}\,d\theta \tag{10A}$$

which can be rewritten as

$$f(x_o,y_o) = -\frac{1}{2\pi^2}\int_{-\frac{\pi}{2}}^{\frac{\pi}{2}}\int_{0}^{\infty}[g(\rho_o+\rho,\theta)+g(\rho_o-\rho,\theta)-2g(\rho_o,\theta)]\frac{d\rho}{\rho^2}d\theta \tag{10B}$$

A Taylor expansion about $\rho = 0$ shows that the integrand in (10B) is well-behaved.

Equation (10B) demonstrates that the controlling parameters for determining the refractive index at a point are the relative phase delays near the point.

VI. NUMERICAL METHOD

A. PROGRAM PARAMETERS

The integration (from $-\pi/2$ to $\pi/2$) over theta yields the same results as integrating over phi from 0 to π[Fig. 3]. The angle, phi equals zero, corresponds to the direction of the parallel rays or viewing angle. The integration over phi is used in order to make the computer program coordinate consistent with the laboratory coordinates.

The FORTRAN IV program developed assumes that all holograms have the same number of equally-spaced data points and that the total number of data points on each plate is odd. A square grid is established over the phase object with spacing determined by spacing of the data points on the holograms at 0 and 90 degrees. The views are assumed to be equally spaced and to cover 180 degrees of view for asymmetric phase objects. Symmetry reduces the necessary field of view until only one view is required for the axi-symmetric case.

To visualize how symmetric fields may be reconstructed from reduced fields of view, consider a phase object of unity refractive index as shown in Figure 14. The field is symmetric about the phi equals zero axis (x axis). The fringe information in the second quadrant is exactly the same as that in the first quadrant. The numerical method developed generates additional data as necessary, depending

on the degree of symmetry. The 180 degree view is in all cases generated by the computer program from the zero degree view by copying the fringe data in reverse order. For a description of input parameters see the computer program.

B. THE INFINITE ρ INTEGRATION

Ideally, $g(\rho,\phi)$ would be zero for ρ greater than RMAX (the radius of the inversion domain). Actual data from a wind tunnel will in some cases have a non-zero fringe shift at RMAX. The method devised to handle the case of non-zero fringe shifts at RMAX expands the fringe data using a cubic polynomial which matches the slope at RMAX and is zero at 2 RMAX. This method is used in all cases since if $g(\rho,\phi)$ is zero at RMAX, the coefficients for the cubic polynomial are zero. For the general case, $g(\rho,\phi)$ is zero for ρ greater than 2 RMAX.

The numerator of the integrand of Equation (10B) $[g(\rho_o+\rho,\phi)+g(\rho_o-\rho,\phi)-2g(\rho_o,\phi)]$ is not a function of ρ for $\rho \geq 3$ RMAX provided that $|\rho_o| \leq$ RMAX. The infinite ρ integration is divided into two regions

$$f(x_o,y_o) = -\frac{1}{2\pi^2}\int_0^{\pi}\int_0^{3RMAX}\frac{g(\rho_o+\rho,\phi)+g(\rho_o-\rho,\phi)-2g(\rho_o,\phi)}{\rho^2}d\rho d\phi$$

$$-\frac{1}{2\pi^2}\int_0^{\pi}\int_{3RMAX}^{\infty}\frac{g(\rho_o+\rho,\phi)+g(\rho_o-\rho,\phi)-2g(\rho_o,\phi)}{\rho^2}d\rho\, d\phi$$

The integrand in the second term reduces to

$$\frac{g(\rho_o+\rho,\phi)+g(\rho_o-\rho,\phi)-2g(\rho_o,\phi)}{\rho^2} = -\frac{2g(\rho_o,\phi)}{\rho^2}$$

because $g(\rho_o+\rho,\phi)+g(\rho_o-\rho,\phi)$ is zero for $\rho \geq 3$ RMAX. Since $g(\rho_o,\phi)$ is not a function of ρ, the integration over ρ may be performed and the second term becomes

$$-\frac{1}{2\pi^2}\int_0^{\pi}\frac{2g(\rho_o,\phi)}{3\ \mathrm{RMAX}}\,d\phi$$

Recombining the two terms, one has

$$f(x_o y_o) = -\frac{1}{2\pi^2}\int_0^{\pi}\left[\int_0^{3\mathrm{RMAX}}\frac{g(\rho_o+\rho,\phi)+g(\rho_o-\rho,\phi)-2g(\rho_o,\phi)}{\rho^2}d\rho + \frac{2g(\rho_o,\phi)}{3\ \mathrm{RMAX}}\right]d\phi \qquad (10C)$$

Figure 12 shows a typical variation of the argument of Equation (10B) versus ρ. The ρ integration from zero to 3 RMAX is performed using Cote's sixth order formulas [Ref. 10].

For the points (x_o,y_o) corresponding to the established grid intersections (Fig. 3), the values of ρ_o correspond to available data points only for the views where phi equals 0 or 90 degrees. For all other views, the value of ρ_o will lie somewhere between two data points. The procedure used calculates the value of the inside integral

$$G(\rho_L,\phi_k) = \int_0^{3RMAX} \frac{g(\rho_L+\rho,\phi_k)+g(\rho_L-\rho,\phi_k)-2g(\rho_L,\phi_k)}{\rho^2}\, d\rho + \frac{2g(\rho_L,\phi_k)}{3\ RMAX}$$

at each data point on each hologram. Hence for each $g(\rho_L,\phi_k)$ there corresponds a function $G(\rho_L,\phi_k)$ which is the inside integral of Equation 10B evaluated at that data point. For a given view ϕ and a given point (x_o,y_o), the corresponding value of ρ_o will be such that $[\rho_L \leq \rho_o \leq \rho_{L+1}]$. A cubic polynomial in ρ is fitted to the points $G(\rho_{L-1},\phi_k)$, $G(\rho,\phi_k)$, $G(\rho_{L+1},\phi_k)$, and $G(\rho_{L+2},\phi_k)$ and the value of $G(\rho_o,\phi_k)$ is obtained by evaluating the cubic polynomial at ρ_o.

If NP is the number of data points for each view and K is the number of views, the inside integral must be evaluated (NP·K) times. For each of the $(NP)^2$ grid intersections there are K interpolations for $G(\rho_o,\phi_k)$ and an integration over phi.

C. THE INTEGRATION OVER PHI

The number of views obtained in actual experiments are usually quite limited. These limited views are the determining factor in the accuracy of the inversion process. It is desirable to achieve a fairly accurate method of integration over phi that does not place undue restrictions on the experimenter.

The integration on phi proceeds from 0 to π; however, the value of the inside integration is known outside this range. Let $G(\phi)$ be the value of the inside integration and $\Delta\phi$ equal the spacing of the views. Then

$$G(0 - \Delta\phi) = G(180 - \Delta\phi)$$

$$G(180 + \Delta\phi) = G(\Delta\phi)$$

By using overlapping parabolas through each succeeding data point with the first parabola centered at phi = 0, the next parabola centered at phi = $\Delta\phi$, etc., the following coefficients result

$$f(x_o,y_o) = -\frac{\Delta\phi}{2\pi^2}\left[\frac{G(0)}{2} + G(\Delta\phi) + \ldots + G(180-\Delta\phi)+\frac{G(180)}{2}\right]$$

which is the trapezoidal rule for integration.

Hence the integration over phi proceeds quite rapidly and no restrictions are placed on the experimenter as to the number of views that must be supplied, except that $\Delta\phi$ must not be too large.

VII. PROGRAM TESTING

A. TEST INVERSIONS

The computer program has the capability of generating the fringe shift information $g(\rho,\phi)$ for an arbitrary refractive index which is supplied by the user. This feature may be used to test the ability of the program to invert various anticipated density fields. The following test refractive index fields were used in MODE 1 (see computer program).

1. Axisymmetric Gaussian

The relative refractive index supplied was

$$f(x,y) = e^{(-x^2-y^2)}$$

with a 2 cm inversion radius. [Figure 4]

2. Axisymmetric Shock

The function supplied was similar to that which would be encountered by a supersonic cone at zero angle of attack.

$$f(x,y) = -.5\sqrt{x^2+y^2} + 2 \qquad R \leq 1.5$$

$$= 0 \qquad R > 1.5$$ [Figure 5]

3. Axisymmetric Shock With Restricted Data

The function was as in (2), except with restricted data which doesn't have a sufficiently large inversion radius.

$$f(x,y) = -.5\sqrt{x^2+y^2} + 2 \qquad R \leq 1.5$$

$$= .25 \qquad 1.5 < R \leq 3.5$$

$$= 0 \qquad R > 3.5$$

[Figures 6 & 7]

4. Asymmetric Gaussian

The relative refractive index was given by

$$f(x,y) = (1 - y^2)\, e^{-x^2} \qquad R \leq 1.2$$

$$= 0 \qquad R > 1.2$$

[Figure 8]

B. INVERSIONS OF ACTUAL DATA

Reference 1 is concerned with the analytical and experimental analysis of an axisymmetric free-jet. Further, the free-jet was tilted to provide a test field which was asymmetric in the plane of the solution. Since the input data files are available in the reference, the same data was used to test the fourier transform method. Three sets of data were used (see input data files).

1. An axisymmetric section at z = .05 cm [Figure 9]

2. An axisymmetric section at z = .5 cm [Figure 10]

3. An asymmetric section at z = .5 cm [Figure 11]

The axisymmetric data consisted of 101 data points at various z locations. Asymmetric data was available at only one position (z = .5) and consisted of nine views with ten degree spacing of the views, and with 60 data points per view. The views covered only 90 degrees since there exists one plane of symmetry for the tilted free-jet.

VIII. DISCUSSION OF RESULTS

A. TEST INVERSIONS

MODE 1 of the computer program artificially generates the g array by performing the line integral of Equation (1B) over the specified relative refractive index [f(x,y)]. In order to reduce quantizing effects of the numerical integration, it was necessary to divide the line integral into 5·np divisions where np is the number of data points from each view. There was little reduction in the quantizing errors when higher order numerical integration techniques were used; therefore, the trapezoidal rule was implemented.

MODE 2 generates the g array from the values of the refractive index which is supplied at the grid points. Although this allows the use of test density fields which cannot be specified analytically, the quantization errors in the g array strongly influence the inversion process. The primary reason for this section of the program is to regenerate the g array for MODE 4 operation (see computer program).

For the axisymmetric case the integration over ϕ is in five degree increments utilizing trapezoidal integration as previously discussed. For the asymmetric case, the views are specified by the user.

1. Axisymmetric Gaussian Inversion

The axisymmetric Gaussian function tests the ability of the program to invert smooth, continuous, axisymmetric

density fields [Fig. 4]. Using 101 data points, the error in the inversion was everywhere less than three per cent of the maximum value of the specified function. The largest errors occurred near the boundaries of the inversion region.

2. Axisymmetric Step Function

The axisymmetric step functions [Fig. 5 & 6] test the ability of the program to invert functions similar to those associated with supersonic flow around axisymmetric shapes. Although the g array is continuous, it has a discontinuity in slope at the step [Fig. 13]. In the continuous case, the integrand of Equation (10C) would become infinite. Because of the discrete nature of the numerical method, the integration over ρ yields a finite value even though it may be quite large if a large number of data points are used [Fig. 13]. The severe properties of the function

$$G(\rho_o,\phi) = \int_0^\infty [g(\rho_o+\rho,\phi)+g(\rho_o-\rho,\phi)-2g(\rho_o,\phi)] \frac{d\rho}{\rho^2}$$

create oscillations and over-shoots in the inversion. It was necessary to introduce an averaging process for the integration over ϕ

$$G(\rho_o,\phi) = \frac{1}{4k\rho_o} \int_{\rho_o-k\Delta\rho}^{\rho_o+k\Delta\rho} S(\rho)\, d\rho$$

where $S(\rho)$ is the third-order polynomial through the four closest values of the inside integral and k is specified by the user ($0 \leq k \leq 1$). This averaging process could be

considered a low pass filter which rejects the higher fourier frequencies. Although the process limits overshoots and oscillations, it also slows the response to the step change in refractive index. The amount of filtering is optional to the user depending on the value of k chosen. There is no filtering if k = 0 and maximum available filtering occurs at k = 1.

With the exception of points near the discontinuity, the maximum errors occur at points external to the step where the maximum error was six per cent of the maximum value of the refractive index. Interior to the shock, the errors in the inversion were on the order of two per cent. The reason for the larger errors outside the step is readily apparent from Figure 13. For a point (x_o,y_o) outside the step function, the phi integration proceeds across the severe portions of the function $G(\phi)$. If the point (x_o,y_o) lies within the step function, the integration over phi never crosses the severe portion of the curve [Fig. 15].

The value of the inversion tends toward the average at the discontinuous points in the function supplied. The amount of filtering used affects the rise distance and overshoot of the inversion at the shock as would be expected of any low-pass filter.

3. Restricted Radial Coverage

Figure 7 demonstrates the feasibility of the smoothing process discussed in Section VI-A. The fringe shift $g(\rho,\phi)$

was computed from the specified function using a radius of 4 cm. Only the data for a radius of 2 cm was used as input for MODE 3 (g array supplied). Except for the region near the boundary of the inversion domain, the resulting inversion showed no degradation from the results of the inversion using the entire g array.

4. Asymmetric Test Case

The asymmetric test function was chosen such that it contained discontinuous regions as well as regions of negative relative refractive index. Six views were generated over the required 90 degrees of view with 101 data points per view. The inversion was accurate to within 5 per cent over the entire domain, except near the discontinuity. The inversion showed good response to the discontinuity [Fig. 8]. The 0 degree cross section shows that the program continuously underestimates the refractive index. A test conducted using the axisymmetric function of Figure 4 as an asymmetric function with the same number of views verified that this is the case. Since the only difference was the number of views available (11 versus 37) for the integration over phi, the phi integration method is believed responsible.

B. INVERSION OF ACTUAL DATA

1. Axisymmetric Free-jet

The input data available from Reference 1 contained 100 data points per hologram. Since it was necessary to have an odd number of data points, an additional data point

was added at $\rho = 0$ by averaging the points on either side. The results of the inversion process were within 3 percent of the results obtained by Matulka [Fig. 9 & 10]. There was evidence of a continuous under-estimation of the density field by the program. The effect of adding one additional point was evident near the origin where the maximum difference in the two solutions occurred. The present program also has a slower response at the boundaries due to the filtering used.

2. Asymmetric Free-jet

An additional data point was added to the available data at $\rho = 0$ to give a total of 61 data points on each of the nine views. The addition of the data point is believed to be the primary cause of the low value for the density at the origin [Fig. 11]. The procedure of adding one data point at the origin by an averaging technique affects not only the value at the origin, but also points near the origin since it is the relative phase delays that are being measured. The reason for the low value of density at points near the origin is not caused by the fact that the interpolated value for the fringe shift at the origin is grossly in error. The error is introduced by the fact that the data from a 60 point spacing is read into a 61 point spacing.

To visualize how this occurs, consider the 1.5 cm radius of inversion used. The grid spacing for 60 data points would be 3.0/59. The grid spacing for 61 data points would be 3.0/60. The two grids correspond exactly at ±RMAX

and deviate by half a grid spacing at the center. This distortion of the resulting inversion can be visualized as a stretching of the density field near the origin which is gradually removed by compression of the density field as one moves toward the boundaries of the density field.

There was a ten percent difference in the two solutions at the origin, and approximately five percent difference at the boundaries of the jet. Again the filtering process slowed the response of the inversion in regions with large gradients.

IX. CONCLUSIONS AND RECOMMENDATIONS

The Fourier transform technique represents considerable savings in computational effort. With appropriate restrictions, it may be used successfully in the analysis of discontinuous density fields. The simplicity of Equation (10B) makes the controlling parameters readily apparent. The integrand of Equation (10B) is related to the rate of change of the slope of the g array. It has been demonstrated that filtering techniques can be implemented that will handle cases involving g arrays with discontinuous slopes. The computer program written has numerous options, is easy to use, and requires little computational time.

The ability of the program to handle discontinuous g arrays, such as might be encountered in studying complex flow patterns, has not been fully documented. It is expected that the filtering method used will handle discontinuous g arrays.

Additional investigation of numerical methods to deal with the problems of discontinuities is warranted. The importance of numerous views around the test section must not be underestimated. Due to the restrictive nature of wind tunnels, it is often difficult to obtain the necessary number of views. Any method which would enable the experimenter to reduce the number of views or decrease the necessary field of view would be invaluable.

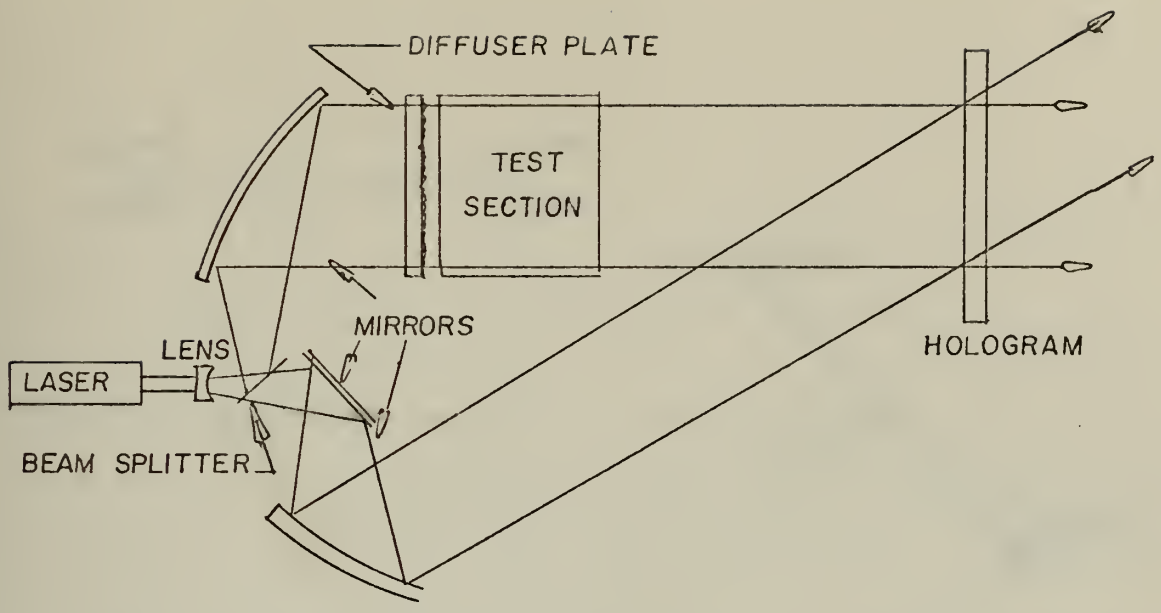

PRODUCTION OF A HOLOGRAM OF A TRANSILLUMINATED OBJECT

FIGURE—1

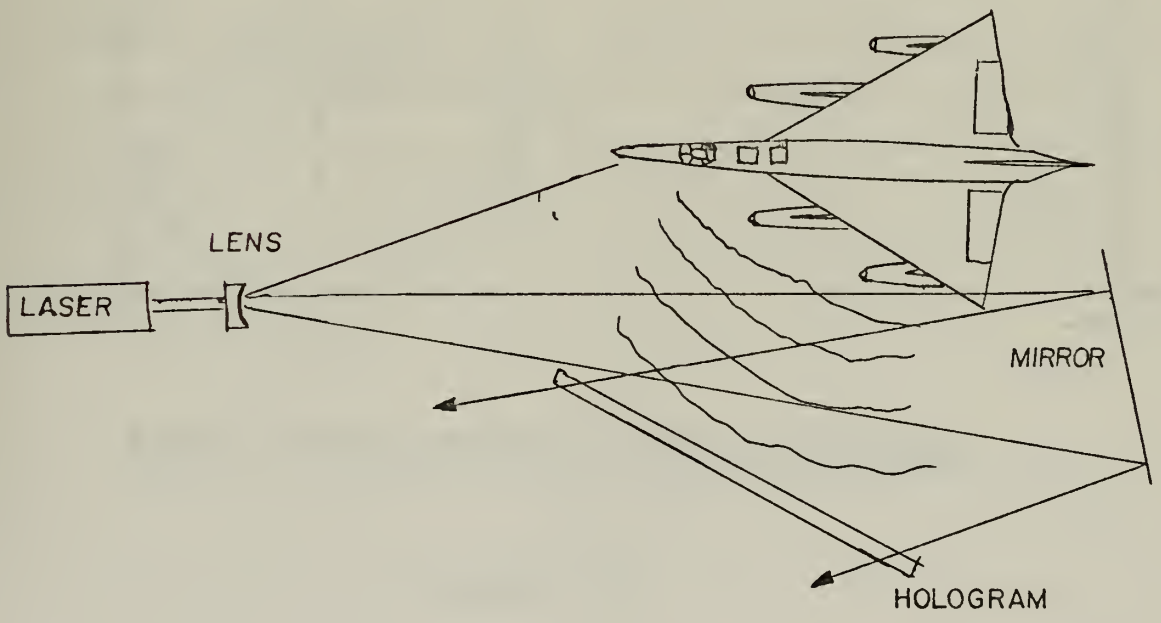

HOLOGRAM OF A DIFFUSELY REFLECTING OBJECT

FIGURE—2

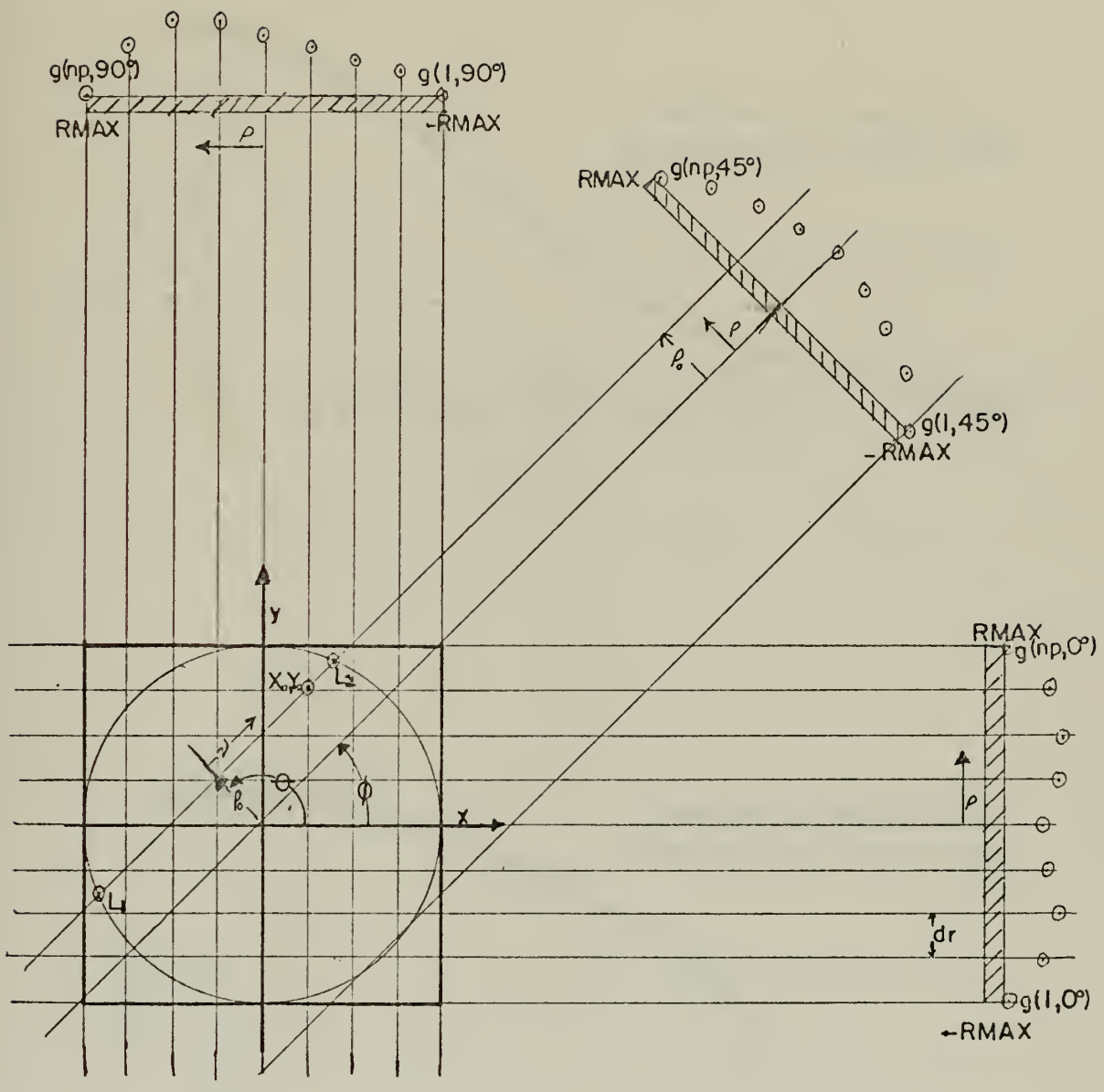

BASIC COORDINATES OF THE INVERSION

FIGURE – 3

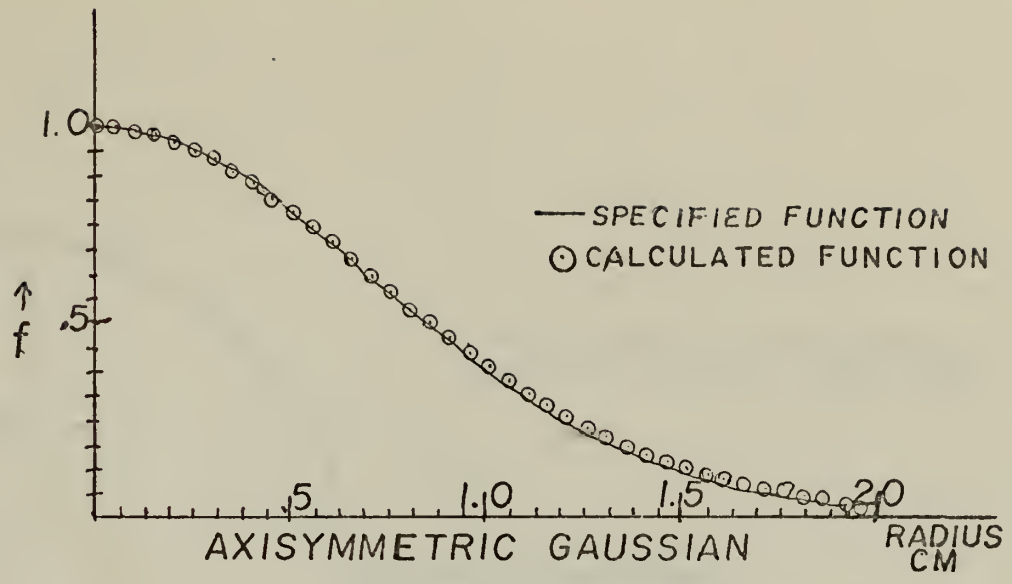

FIGURE-4

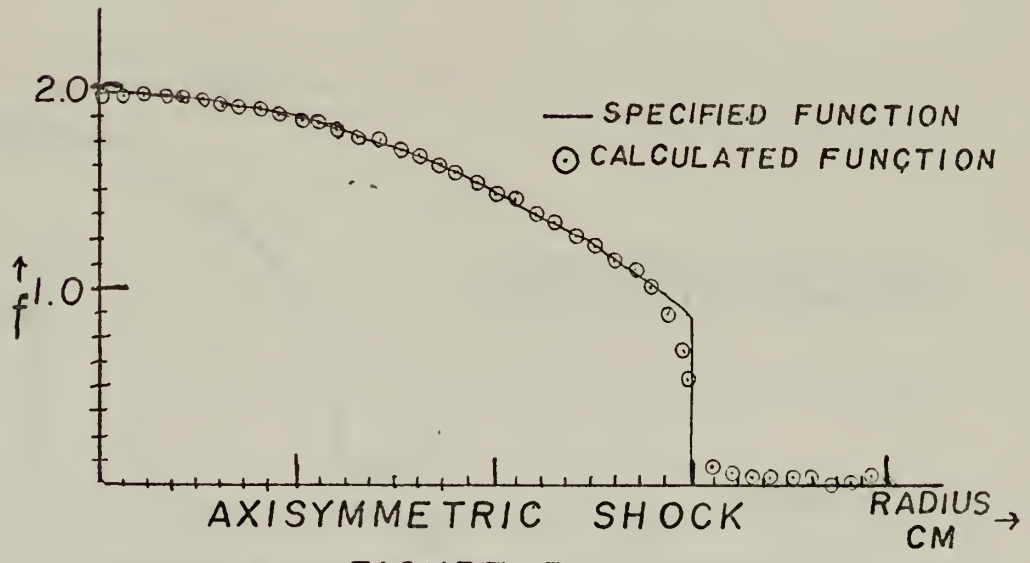

FIGURE-5

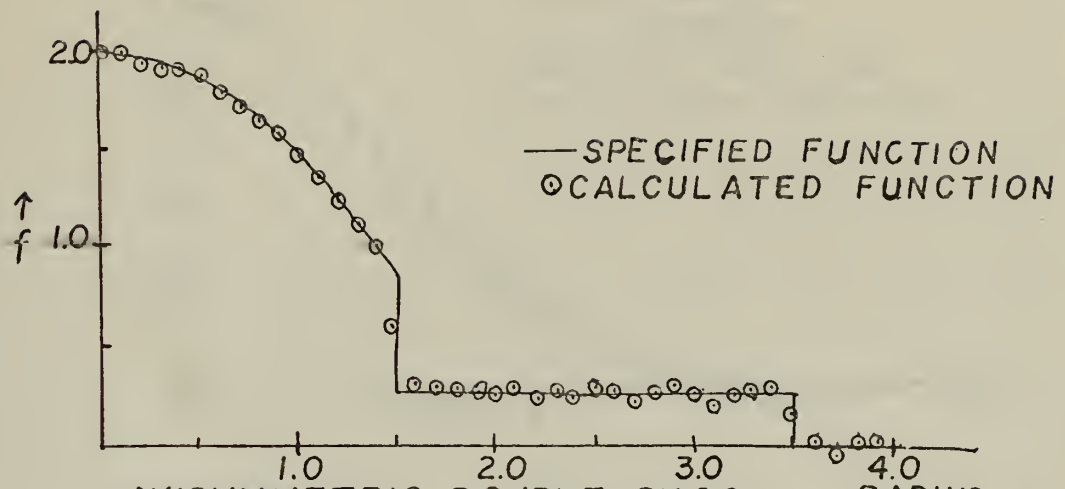

AXISYMMETRIC DOUBLE SHOCK

FIGURE-6

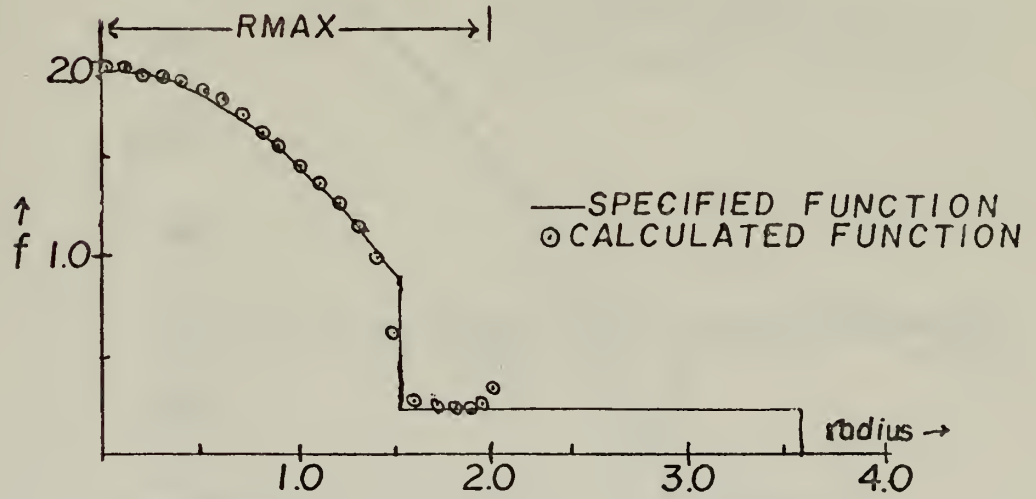

INCOMPLETE FRINGE COVERAGE

FIGURE-7

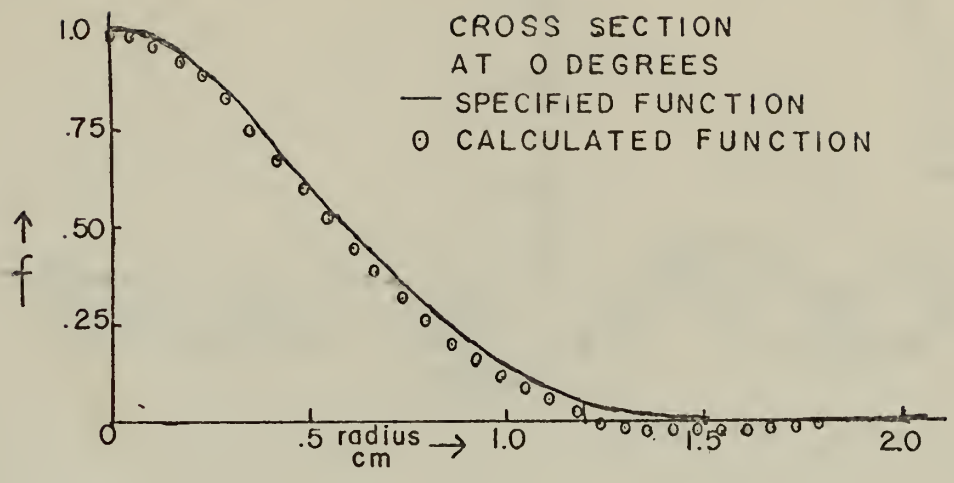

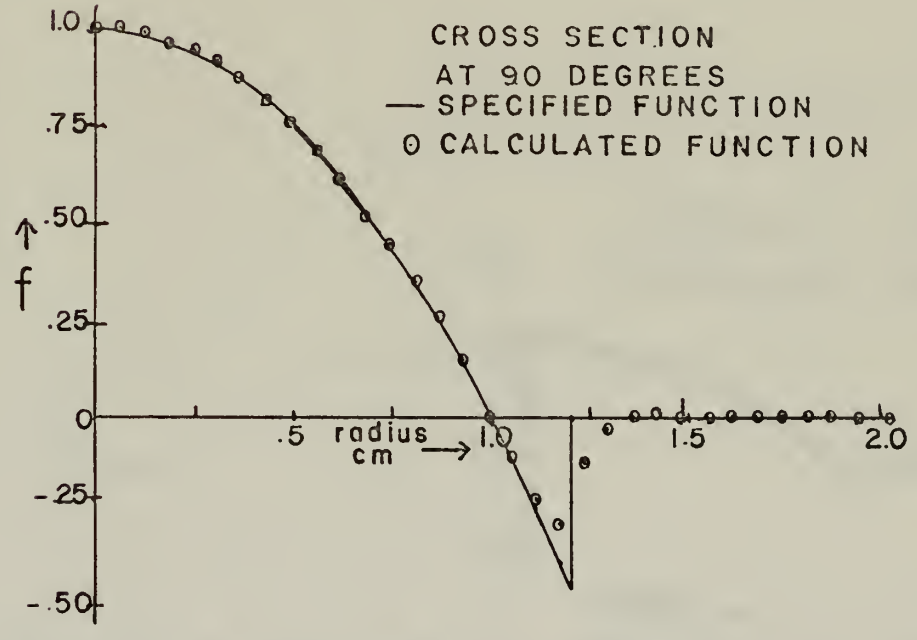

ASYMMETRIC TEST CASE
FIGURE – 8

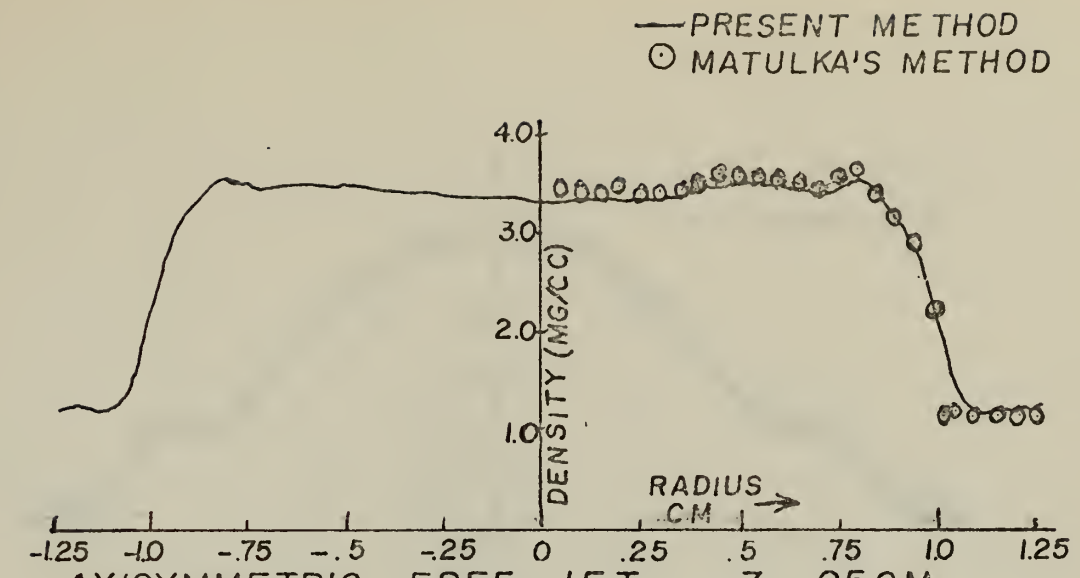

AXISYMMETRIC FREE JET Z = .05CM

FIGURE - 9

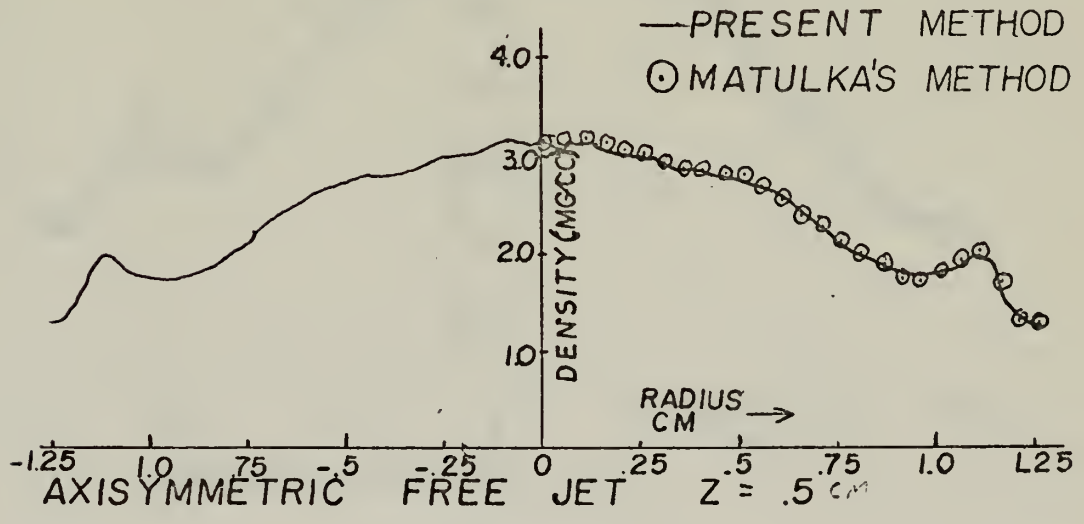

AXISYMMETRIC FREE JET Z = .5 CM

FIGURE - 10

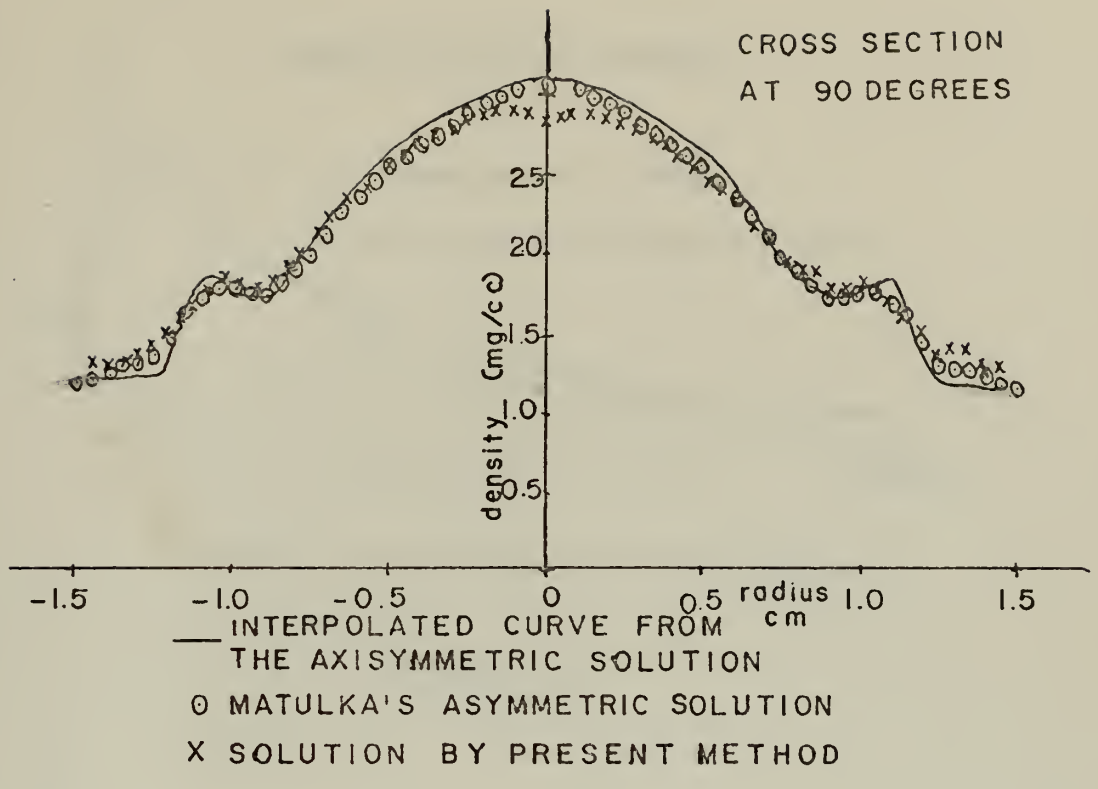
CROSS SECTION
AT 90 DEGREES
density (mg/cc)
2.5
2.0
1.5
1.0
0.5
-1.5
-1.0
-0.5
0
0.5
1.0
1.5
radius cm
INTERPOLATED CURVE FROM THE AXISYMMETRIC SOLUTION
0 MATULKA'S ASYMMETRIC SOLUTION
X SOLUTION BY PRESENT METHOD

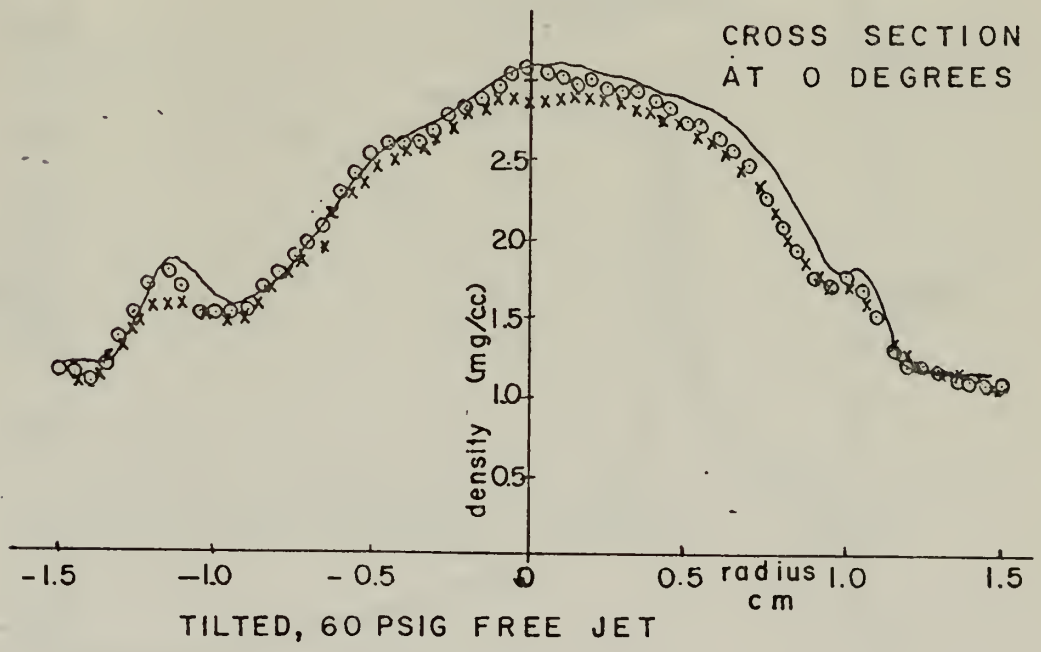
CROSS SECTION
AT 0 DEGREES
density (mg/cc)
2.5
2.0
1.5
1.0
0.5
-1.5
-1.0
-0.5
0
0.5
1.0
1.5
radius cm
TILTED, 60 PSIG FREE JET

FIGURE—11.

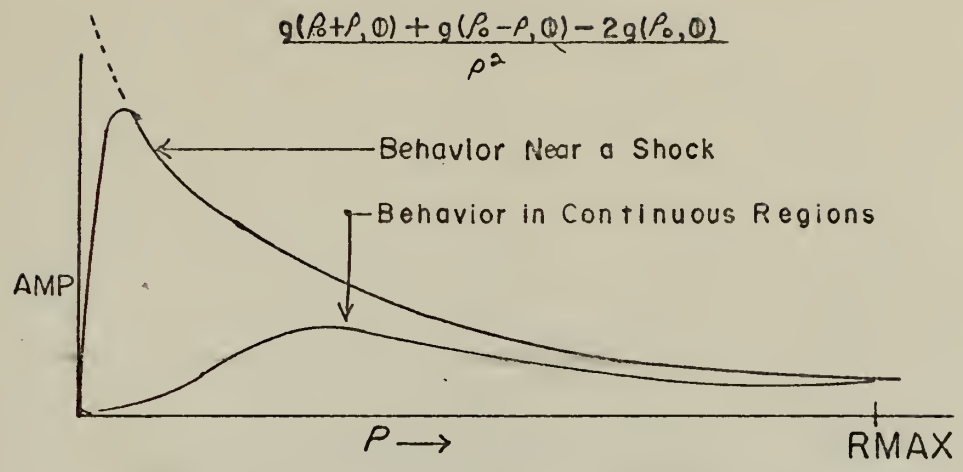

TYPICAL VARIATION OF INTEGRAND

FIGURE—12

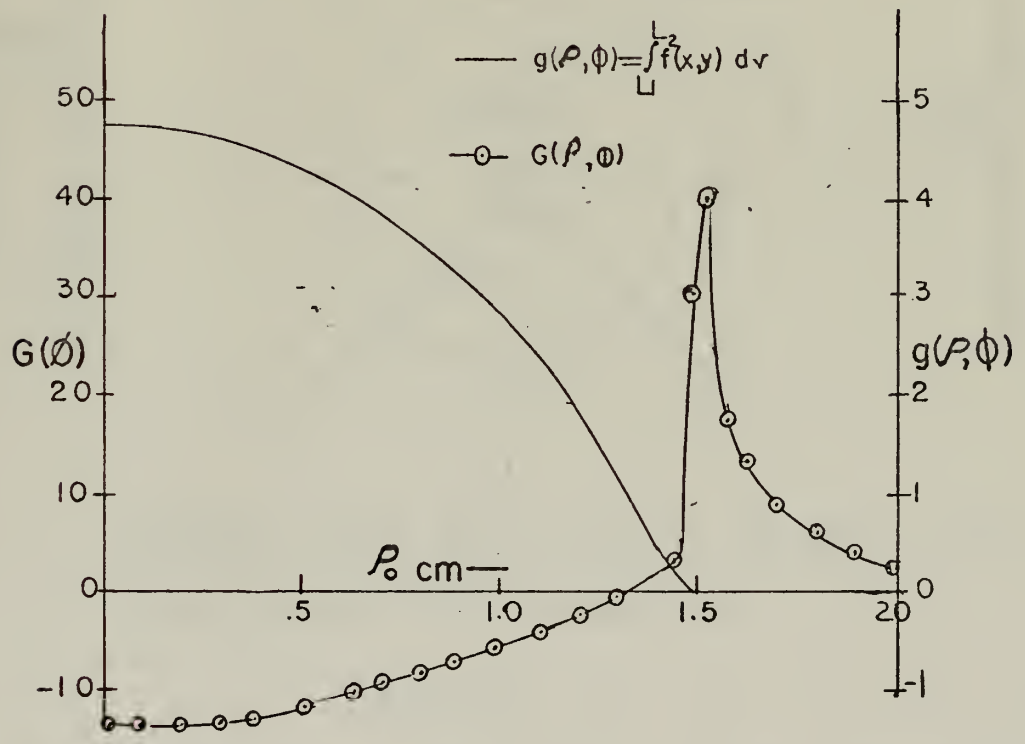

FRINGE SHIFT AND VALUE OF THE INSIDE INTEGRAL FROM THE AXISYMMETRIC SHOCK

FIGURE —13

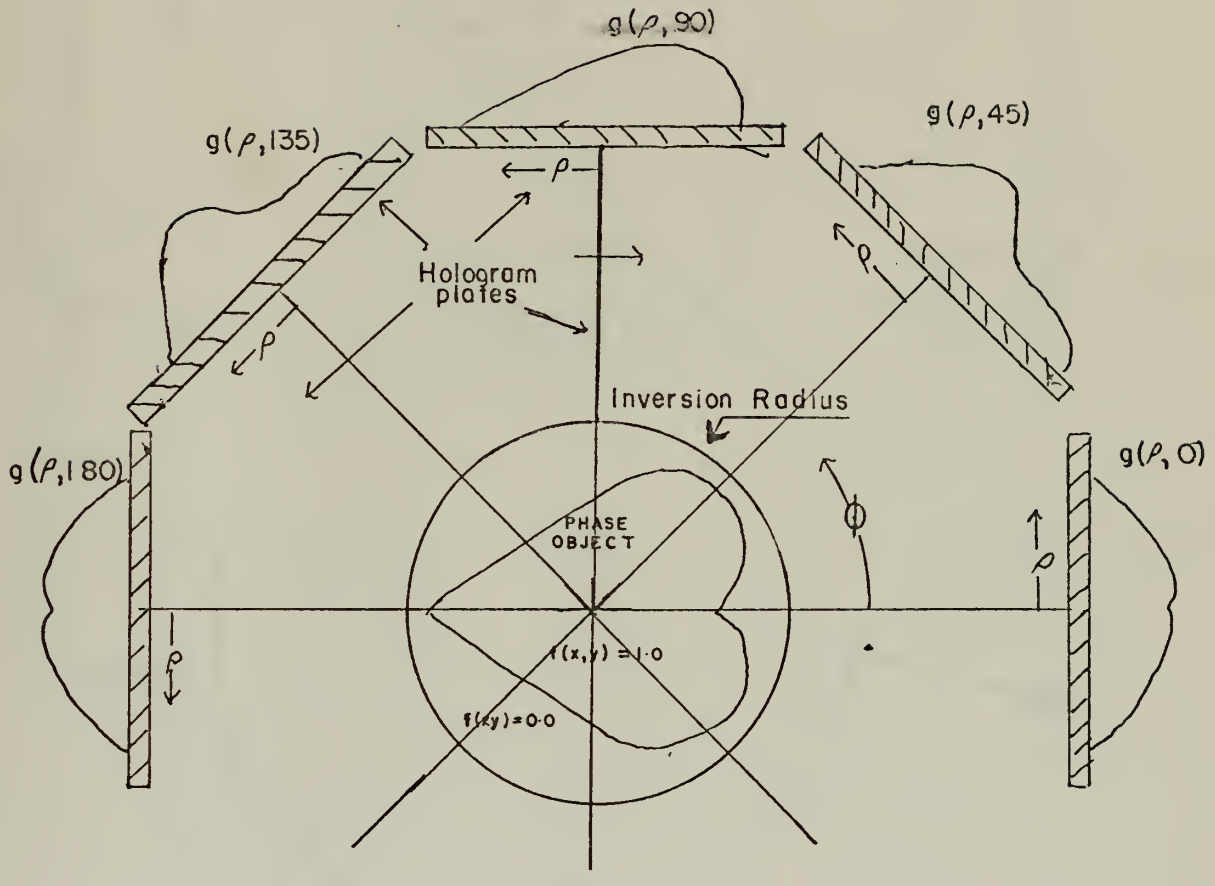

FRINGE DATA OF A PHASE OBJECT WITH ONE DEGREE OF SYMMETRY

FIGURE-14

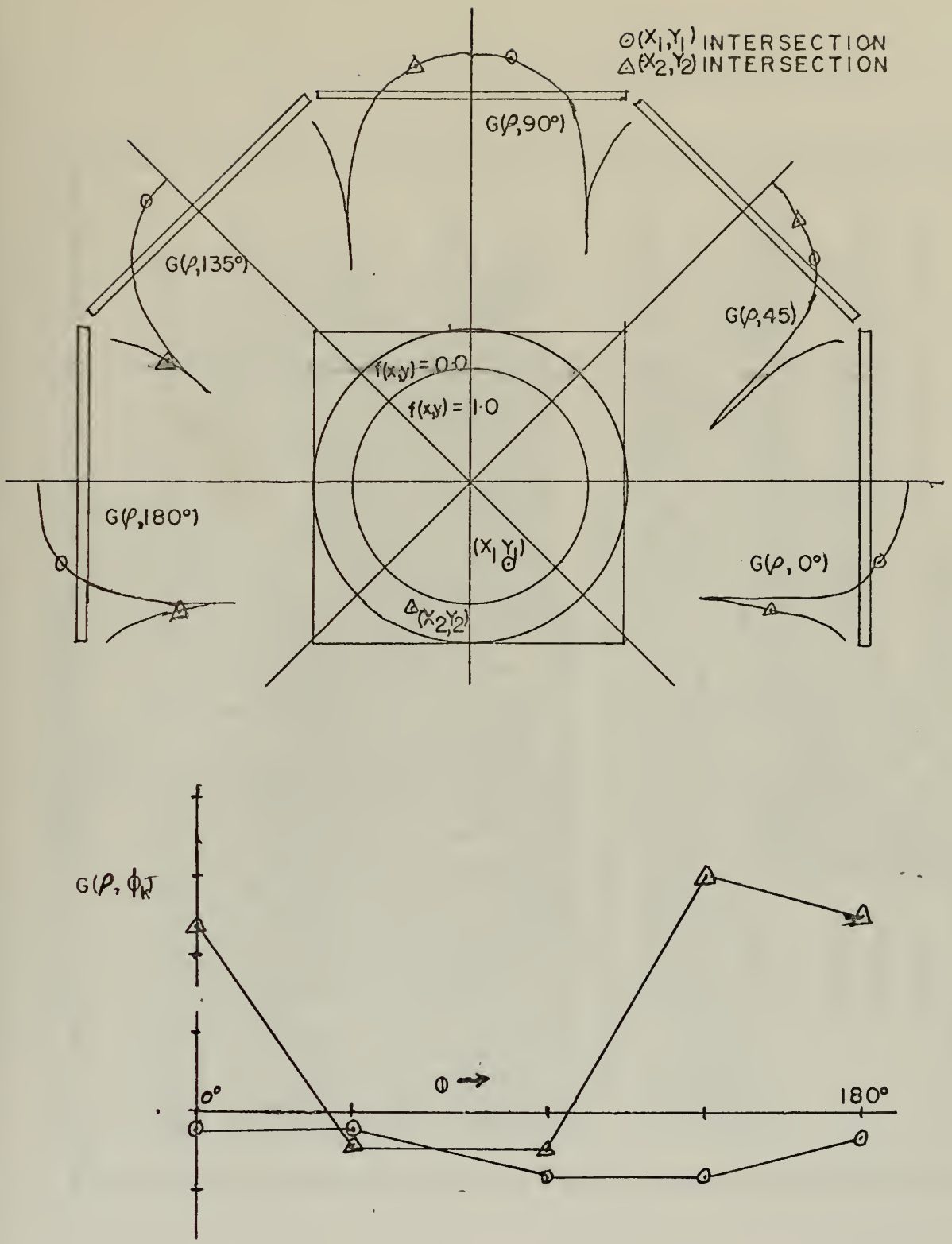

FIGURE 15 $G(\rho_L, \phi_K)$ for Points (X_0, Y_0) from an Axisymetric STEP Function

COMPUTER PROGRAM

```
C     ************************************************************
C     *                                                          *
C     *                    INTEGRAL INVERSION                    *
C     *                                                          *
C     *  REFERENCE, THESIS BY P. E. VAN HOUTEN 'THE APPLICATION OF   *
C     *  HOLOGRAPHIC INTERFEROMETRY TO THE DETERMINATION OF DISCON-  *
C     *  TINUOUS THREE-DIMENSIONAL DENSITY FIELDS' 14 DEC 72         *
C     *       THE PROGRAM CONSIDERS A CIRCULAR REGION OF UNKNOWN     *
C     *  REFRACTIVE INDEX FOR WHICH THE TOTAL PHASE SHIFT(PATH LENGTH*
C     *  DIFFERENCE) IS KNOWN FOR NUMEROUS RAYS AT REGULAR INTERVALS *
C     *  FOR A GIVEN VIEWING ANGLE. THE PROGRAM REQUIRES NUMEROUS    *
C     *  VIEWS AT REGULARLY SPACED INTERVALS AND A TOTAL ANGULAR     *
C     *  COVERAGE OF 180 DEGREES(ASYMMETRIC). THE NECESSARY ANGULAR  *
C     *  COVERAGE IS REDUCED BY THE NUMBER OF DEGREES OF SYMMETRY.   *
C     *  BY THE USE OF TWO DIMENSIONAL FOURIER TRANSFORM TECHNIQUES  *
C     *  IT CAN BE SHOWN THAT  FOR A GIVEN POINT(XO,YO) WITHIN THE   *
C     *  CIRCULAR REGION, THE DENSITY F(XO,YO) CAN BE EXPRESSED IN   *
C     *  TERMS OF THE PHASE SHIFT INFORMATION G(RO,THETA).           *
C     *       IN ORDER TO SAVE COMPUTATION TIME, THE VALUE OF THE    *
C     *  INSIDE INTEGRATION IS COMPUTED AT EACH RAY POSITION FOR EACH*
C     *  VIEWING ANGLE. FOR A GIVEN POINT(XO,YO), THE VALUE OF THE   *
C     *  INSIDE INTEGRAL IS DETERMINED BY AVERAGING OVER A FINITE    *
C     *  PORTION OF A CUBIC POLYNOMIAL FITTED TO THE FOUR CLOSEST    *
C     *  VALUES OF THE INSIDE INTEGRAL.  THE INTEGRATION OVER THETA  *
C     *  USES THE TRAPEZOIDAL RULE.  THE INTEGRATION OVER RHO USES   *
C     *  COTES SIXTH ORDER QUADATURE FORMULA                         *
C     *                                                          *
C     *     MEANING OF SYMBOLS USED IN THE PROGRAM               *
C     *                                                          *
C     *  IT(12)  TITLE USED FOR OUTPUT.  FIRST 48 CHARACTERS ON FIRST*
C     *          DATA CARD, FIRST 16 CHARACTERS ON NEXT DATA CARD    *
C     *  RHOINF-DENSITY OUTSIDE REGION OF INTEREST IN MG/CC.         *
C     *  XLAMDA-WAVELENGTH OF MONOCHROMATIC,COHERENT LIGHT SOURCE IN *
C     *  MICRONS.                                                    *
C     *  RHOINF AND XLAMDA ON THIRD DATA CARD IN (2F10.5) FORMAT     *
C     *  MODE      MODE=1  REFRACTIVE INDEX SUPPLIED THROUGH SUBROUTINE*
C     *                    'INPUT'. THE PROGRAM GENERATES FRINGE DATA*
C     *                    AND RECOMPUTES THE REFRACTIVE INDEX FROM  *
C     *                    THE GENERATED FRINGE DATA.                *
C     *            MODE=2  REFRACTIVE INDEX SUPPLIED AT GRID POINTS  *
C     *                    BY INPUT DATA. PROGRAM PROCEEDS AS IN MODE 1*
C     *            MODE=3 FRINGE DATA SUPPLIED, PROGRAM GENERATES    *
C     *                   DENSITY FIELD.                             *
C     *            MODE=4  SAME AS MODE=3 EXCEPT FRINGE DATA IS RECOM-*
C     *                    PUTED AS PER MODE =2.                     *
C     *  NP  NUMBER OF EQUALLY SPACED DATA POINTS                    *
C     *  NT  NUMBER OF VIEWS SUPPLIED                                *
```

```
C      *  KSYM  SYMMETRY OF FIELD  0-4 AXIS OF SYMMETRY                    *
C      *                             4 -98  DATA REPEATS EVERY KSYM       *
C      *                                    DEGREES.                      *
C      *                            99 AXISYMETRIC FIELD                  *
C      *  RMAX  RADIUS OF CIRCULAR REGION  IN CENTIMETERS                 *
C      *  FILTER = (0.-1.) DETERMINES SPAN OVER WHICH AVERAGING OCCURS    *
C      *  THE ABOVE INFORMATION ON THE FOURTH DATA CARD(4I10,2F10.5).     *
C      *  X(I)   VECTOR OF GRID POINTS ALONG THETA = 0 DEGREES            *
C      *         X(1)=-RMAX     X(NP)=+RMAX                              *
C      *  Y(J)   VECTOR OF GRID POINTS ALONG THETA=90 DEGREES             *
C      *         Y(1)=-RMAX   Y(NP)=+RMAX                                 *
C      *  A(I,J)   DENSITY OR REFRACTIVE INDEX AT THE POINT X(I),Y(J).    *
C      *  RB(I) VECTOR OF POINTS ON THE HOLOGRAPHIC PLATE RB(1)=-2 RMAX   *
C      *  RB(2 NP)=2 RMAX.          -                                     *
C      *  DR   SPACING OF GRID,SPACING OF RAYS.  DR=2*RMAX/(NP-1)         *
C      *  TH(K)   VECTOR OF VIEWING ANGLES  IN DEGREES                    *
C      *  B(I,K)   FRINGE SHIFT INFORMATION AT THE POINT(RB(I),TH(K)).    *
C      *  B(I,K) IS COPIED INTO BB(I,K). THE VALUE OF THE INSIDE          *
C      *  INTEGRATION IS THEN STORED IN B(I,K).                           *
C      *  DASYM(K) SYMMETRY OF DATA(B(I,K). 0 NO SYMETRY                  *
C      *                                    1 DATA SYMETRIC ABOUT RB=0.   *
C      *  IF DASYM = 1.0 ONLY (NP+1)/2 DATA POINTS SHOULD BE FURNISHED.   *
C      *  BD(L) IS A WORK VECTOR USED BY THE PROGRAM.                     *
C      *  FOR MODE=1 OR  MODE=2 THE FIFTH DATA CARD IS THE VECTOR         *
C      *  TH(K) IN (8F10.5) FORMAT                                        *
C      *  FOR MODE 2 OPERATION THE REFRACTIVE INDEX FOLLOWS IN 8F10.5     *
C      *  FORMAT.                                                         *
C      *  FOR MODE=3 AND MODE=4 OPERATION, THE FIFTH DATA CARD IS         *
C      *  TH(1) AND DASYM(1) IN (2F10.5) FORMAT.  THIS IS FOLLOWED        *
C      *  BY THE FRINGE INFORMATION FOR THAT VIEW (B(I,1) ETC UNTIL       *
C      *  ALL VIEWS AND FRINGE SHIFT HAS BEEN SUPPLIED                    *
C      *  IF AXIS OF SYMMETRY EXISTS,THETA=0. MUST CORRESPOND TO ONE OF   *
C      *  THE AXIS OF SYMMETRY.                                           *
C      *                                                                  *
C      ********************************************************************
       REAL*8 IT(12),LAB,ITSUB(12)/'REFRACTIVE INDEXDENSITY IN MG/CC     T
      1HETA=  0DEG    THETA= 90DEG    THETA= 45DEG    THETA=-45DEG'/
       DIMENSION X(151),Y(151),A(151,151),B(151,20),BD(811),TH(36),
      1BB(301,20),RB(301),DASYM(20),SS(36),CC(36)
       F1(AA,BD,CC,RR)=CC+RR*(BD+RR*(AA))
       DATA C1,C2,C3,C4/.2292857,1.54285,.192857,1.94285/,LAB/'          '/
  100 FORMAT (4I10,2F10.5)
  101 FORMAT('0',T20,'   MODE     NUM PTS  NUM VIEWS   KSYM   RADIUS
     1GRID SPACING  FILTER')
  102 FORMAT('0',T17,4I10,3F10.5)
  103 FORMAT(8F10.5)
  104 FORMAT('0',T7,20F6.1//)
  105 FORMAT('0',F5.2,20F6.2)
```

```
  106 FORMAT('0',//)
  107 FORMAT('0',T9,'MODE 1',T26,'MODE 3',T45,'VALUE'/,T9,'GIVEN    COMP
     1    DENSITY',T47,'OF'/,'RADIUS  REFRAC   REFRAC  FIELD      FRINGE
     2  INSIDE'/,'  CM    INDEX    INDEX   MG/CC      SHIFT     INTEGRAL'
     3//)
  108 FORMAT('0',T20,'RHOINF =',F7.5,' MG/CC  LAMDA=',F7.5,' MICRONS')
  110 FORMAT('1',T7,21F6.2//)
  111 FORMAT('0',F5.2,1X,21F6.2)
  112 FORMAT(6A8)
  113 FORMAT(' ',T40,'Y AXIS(THETA=90 DEGREES) VERTICAL'/,T40,
     1'X AXIS(THETA = 0 DEGREES) HORIZONTAL'//)
  114 FORMAT('0',T40,'DENSITY FIELD IN MG/CC FOLLOWS')
  115 FORMAT('0',T40,'INDEX OF REFRACTION FOLLOWS')
  116 FORMAT('1','THE EXPANDED FRINGE SHIFT INFORMATION IS AS FOLLOWS'/)
  117 FORMAT('1','THE VALUE OF THE INSIDE INTEGRATION IS AS FOLLOWS'//)
  118 FORMAT(10F7.4)
      READ(5,112) (IT(I),I=1,12)
      READ(5,103) RHOINF,XLAMD
      READ(5,100) MODE,NP,NT,KSYM,RMAX,FILTER
      WRITE(6,108) RHOINF,XLAMD
      FNP=FLOAT(NP)
      DR=2.*RMAX/(FNP-1)
      WRITE(6,101)
      WRITE(6,102) MODE,NP,NT,KSYM,RMAX,DR,FILTER
      N=(NP+1)/2
      NPL=(NP-1)/2
      NPP=2*NP-1
      MAX=NP+NPL
      RM2=RMAX**2
      NP5=3*NP-2
      FNP5=FLOAT(NP5)
      NPM1=NP-1
      FT2=FILTER*FILTER
C
C*****ZERO MATRICES AND SET GRID ************************************
C
      DO 2 I=1,NP
      DO 1 J=1,NP
    1 A(I,J)=0.0
      DO 2 K=1,NT
    2 B(I,K)=0.0
      X(1)=-RMAX
      Y(1)=X(1)
      DO 3 I=2,NP
      X(I)=X(I-1)+DR
    3 Y(I)=X(I)
C
C*********************************************************************
```

```
      GO TO (4,4,29,29),MODE
C
C*****READ VIEWING ANGLES AND SET SIN AND COSINE FOR MODE=1,2**********
C
    4 READ(5,103) (TH(K),K=1,NT)
      DO 5 K=1,NT
      THETA=TH(K)/57.296
      CC(K)=COS(THETA)
    5 SS(K)=SIN(THETA)
C
C*************************************************************************
C
      IF(MODE.EQ.1) GO TO 7
C
C*****READ REFRACTIVE INDEX FOR MODE=2 OPERATION**************************
C
      DO 6 I=1,NP
    6 READ (5,103) (A(I,J),J=1,NP)
C
C*************************************************************************
C
      GO TO 9
    7 IF(KSYM.EQ.99) GO TO 13
C
C*****SET REFRACTIVE INDEX AND WRITE SAME FOR MODE ONE OPERATION*******
C
      DO 8 I=1,NP
      DO 8 J=1,NP
      XI=X(I)
      YJ=Y(J)
      CALL INPUT(XI,YJ,VAL)
    8 A(I,J)=VAL
    9 WRITE(6,115)
      WRITE(6,113)
      K=1
      K21=21
   11 WRITE(6,106)
      WRITE(6,110) (X(I),I=K,K21)
      DO 12 I=1,NP
      NN=NP-I+1
   12 WRITE(6,111) Y(NN),(A(J,NN),J=K,K21)
      IF(K21.EQ.NP) GO TO 15
      K=K21+1
      K21=K21+21
      IF(K21.GT.NP) K21=NP
      GO TO 11
```

```
C*************************************************************************
C
C*****SET REFRACTIVE INDEX FOR AXISYMETRIC CASE************************
C
   13 DO 14 I=1,NP
   14 CALL INPUT(X(I),0,A(I,N))
C
C*************************************************************************
C
   15 IF(MODE.EQ.2) GO TO 19
C
C*****INTEGRATE FOR FINGE SHIFT FOR MODE ONE CASE**********************
C
      DO 18 K=1,NT
      R=-RMAX
      B(1,K)=0.0
      B(NP,K)=0.0
      DO 18 I=2,NPM1
      R=R+CR
      P1=SQRT(RM2-R**2)
      DP=2.*P1/FNP5
      P=-P1
      DO 16 J=1,NP5
      YJ=R*CC(K)+P*SS(K)
      XI=-R*SS(K)+P*CC(K)
      CALL INPUT(XI,YJ,VAL)
      P=P+DP
   16 BD(J)=VAL
      SUM=0.
      NPP2=NP5-2
      DO 17 J=1,NPP2,2
C*****INTEGRATION USES SIMPSON'S RULE *********************
   17 SUM=SUM+BD(J)+4.*BD(J+1)+BD(J+2)
   18 B(I,K)=SUM*DP/3.
      GO TO 34
C
C*************************************************************************
C
C*****INTEGRATE FOR FINGE SHIFT FOR MODE TWO CASE**********************
C
   19 K=0
   20 K=K+1
      IF(K.GT.NT) GO TO 33
      IF(TH(K).EQ.0.) GO TO 23
      IF(TH(K).EQ.90.) GO TO 26
      R=-RMAX
      B(1,K)=0.0
      B(NP,K)=0.0
```

```
      DO 22 L=2,NPM1
      SUM=0.
      R=R+DR
      P1=SQRT(RM2-R**2)
      DP=2.*P1/FNP5
      P=-P1
      DO 21 LL=1,NP5
      XN=-R*SS(K)+P*CC(K)
      YN=R*CC(K)+P*SS(K)
C     LINEAR INTERPOLATE FOR VALUE OF REFRACTIVE INDEX*****
      I=(XN+RMAX+DR)/DR
      J=(YN+RMAX+DR)/DR
      XD=(XN-X(I))/DR
      YD=(YN-Y(J))/DR
      VAL=A(I,J)+XD*(A(I+1,J)-A(I,J))
      VAL=VAL+YD*(A(I,J+1)+XD*(A(I+1,J+1)-A(I,J+1))-VAL)
C     ************************************************
      SUM=SUM+VAL*DP
   21 P=P+DP
   22 B(L,K)=SUM
      GO TO 20
   23 DO 25 J=1,NP
      B(J,K)=0.0
      DO 24 I=2,NP
   24 B(J,K)=B(J,K)+ (A(I-1,J)+A(I,J))
   25 B(J,K)=DR*B(J,K)/2.
      GO TO 20
   26 DO 28 I=1,NP
      L=NP+1-I
      B(L,K)=0.0
      DO 27 J=2,NP
   27 B(L,K)=B(L,K)+A(I,J-1)+A(I,J)
   28 B(L,K)=DR*B(L,K)/2.
      GO TO 20
C
C*************************************************************
C
C
C*****READ DATA FOR MODE THREE OR FOUR OPERATION**************
C
   29 DO 32 I=1,NT
      READ(5,103) TH(I),DASYM(I)
      IF(DASYM(I).EQ.1.) GO TO 30
      READ(5,103) (B(J,I),J=1,NP)
      GO TO 32
C     READ AND COPY SYMETRIC DATA **************************
   30 READ(5,103) (B(J,I),J=1,N)
      L=N+1
```

```
      DO 31 J=L,NP
      K=NP-J+1
   31 B(J,I)=B(K,I)
C     **********************************************
   32 CONTINUE
C
C*****************************************************************
C
   33 IF(MODE.EQ.5) GO TO 63
C
C*****SET RADIUS VECTOR AND EXTEND FRINGE INFORMATION TO TWICE RMAX****
C
   34 RB(1)=-2.*RMAX
      DO 35 I=2,NPP
   35 RB(I)=RB(I-1)+DR
      DO 38 I=1,NT
      Q1=B(1,I)
      Q2=(B(2,I)-B(1,I))/DR
      CALL COEF(Q1,Q2,-RMAX,E,G,C)
      DO 36 J=1,NPL
   36 BB(J,I)=F1(E,G ,C,RB(J))
      DO 37 K=1,NP
   37 BB(K+NPL,I)=B(K,I)
      Q1=B(NP,I)
      Q2=(B(NP,I)-B(NP-1,I))/DR
      CALL COEF(Q1,Q2, RMAX,E,G,C)
      L=NP+NPL
      DO 38 K=L,NPP
   38 BB(K,I)=F1(E,G ,C,RB(K))
C
C*****************************************************************
C
C
C*****CALCULATE VALUE OF INSIDE INTEGRAL ******************************
C
      DO 43 I=1,NT
      DO 43 J=1,NP
      M=NPL+J
      BD(1)=0.
      DO 39 K=1,MAX
      MKP=M+K
      MKM=M-K
      IF(MKP.GT.NPP) MKP=NPP
      IF(MKM.LT.1) MKM=1
      K1=K**2
   39 BD(K+1)=(BB(MKP,I)+BB(MKM,I)-2.*BB(M,I))/(FLOAT(K1)*DR)
      VAL=0.
      K1=1
```

```
   40 K2=K1+6
      IF(K2.GT.MAX) GO TO 41
C     COTES SIXTH ORDER QUADATURE FORMULA*****************
      VAL=VAL+C1*(BD(K1)+BD(K2))+C2*(BD(K1+1)+BD(K2-1))+C3*(BD(K1+2)+BD(
     1K2-2))+C4*BD(K1+3)
      K1=K2
      GO TO 40
   41 SUM=0.
C     CONTRIBUTION OF LAST TERMS
      DO 42 K=K1,MAX
   42 SUM=SUM+BD(K)+BD(K+1)
C     SUM COTES PLUS LAST TERMS PLUS INTEGRATION FROM 2 RMAX TO INFINITY
   43 B(J,I)= VAL+SUM/2.-.666667*BB(M,I)/RMAX
      IF(KSYM.LT.99) GO TO 48
C
C**************************************************************************
C
C
C*****INTEGRATE OVER THETA FOR AXISYMETRIC CASE*********************
C
      DEL=-.004421
      M=1
      TH(1)=0.0
      SS(1)=0.0
      DO 44 I=2,19
      TH(I)=TH(I-1)+5.
   44 SS(I)=SIN(TH(I)/59.296)
      WRITE(6,107)
      DO 47 I=1,NP
      DO 45 K=1,19
      R=-X(I)*SS(K)
      L=(R+RMAX+DR)/DR
      IF(L.GE.NP) GO TO 460
      IF(L.LT.1) GO TO 460
      LP2=L+2
      LP1=L+1
      LM1=L-1
      IF(LP2.GT.NP) LP2=NP
      IF(LM1.LT.1) LM1=1
      P=(R-X(L))/DR
      COF3=.1666666*(B(LP2,K)-B(LM1,K))-.5*(B(LP1,K)-B(L,K))
      COF2=.5*(B(LP1,K)+B(LM1,K))-B(L,K)
      COF1=-.1666666*B(LP2,K)+B(LP1,K)-.333333*B(LM1,K)-.5*B(L,K)
      P2=P*P
C*****AMOUNT OF FILTERING DEPENDS ON FT2=FILTER*FILTER**********
   45 BD(K)=P*(P2+FT2)*COF3+(P2+.666666*FT2)*COF2+P*COF1+B(L,K)
      SUM=0.0
```

```
C      TRAPEZOIDAL INTEGRATION ON THETA    ******************
       DO 46 K=2,19
       SUM=SUM+BD(K)+BD(K-1)
   46  CONTINUE
       A(I,1)=SUM*DEL
  460  CONTINUE
C      OUTPUT IS DENSITY FIELD IF MODE=3*********************
       IF(MODE.LT.3) GO TO 47
       A(I,2)=RHOINF+.4443*XLAMD*A(I,1)
   47  WRITE(6,105) X(I),A(I,N),A(I,1),A(I,2),BB(NPL+I,1),B(I,1)

C*****************************************************************
C
C
C*****PLOT AXISYMETRIC DENSITY FIELD*******************************
C
C      REFRACTIVE INDEX SUPPLIED*****************************
       CALL DRAW(NP,X,A(1,1),1,0,LAB,IT,0,0,0,0,0,0,9,3,0,LAST)
C      REFRACTIVE INDEX CALCULATED***************************
       CALL DRAW(NP,X,A(1,N),3,0,LAB,IT,0,0,0,0,0,0,9,3,0,LAST)
       IF(MODE.LT.3) GO TO 75
C      DENSITY FIELD CALCULATED******************************
       CALL DRAW(NP,X,A(1,2),0,0,LAB,IT,0,0,0,0,0,0,9,3,0,LAST)
C
C*****************************************************************
C
       GO TO 75
   48  M=NT+1
       IF(KSYM.EQ.0) GO TO 51
       IF(KSYM.GT.4) GO TO 53
C
C*****GENERATE ADDITIONAL DATA DEPENDING ON SYMETRY OF FIELD*******
C
       DT=TH(2)-TH(1)
       NTP=NT
       DO 50 J=1,KSYM
       K=J*NT
       DO 49 I=1,NTP
       KK=K+I
       TH(KK)=TH(KK-1)+DT
       KM=K-I+1
       DO 49 L=1,NP
   49  B(L,KK)=B(L,KM)
   50  NTP=2*NTP
       M=KK+1
C
C*********************************************************************
```

```
C*****GENERATE DATA FOR 180 DEGREE VIEW*******************************
C
   51 TH(M)=TH(1)+180.
      DO 52 I=1,NP
      K=(NP-I+1)
   52 B(K,M)=B(I,1)
C
C**************************************************************************
C
      GO TO 55
C
C*****GENERATE ADDITIONAL DATA FOR REPEATING DATA**********************
C
   53 M=180/KSYM+1
      DO 54 I=2,M
      TH(I)=TH(I-1)+FLOAT(KSYM)
      DO 54 J=1,NP
   54 B(J,I)=B(J,I-1)
   55 CONTINUE
C
C**************************************************************************
C
C
C*****INTEGRATE ON THETA FOR ASYMETRIC FIELD***************************
C
      MD=M-1
      DEL=-1./(2.*3.1416*FLOAT(MD))
      DO 56 I=1,M
      CC(I)=COS(TH(I)/59.296)
   56 SS(I)=SIN(TH(I)/59.296)
      DO 61 LL= 1,NP
      J=NP+ 1-LL
      DO 60 I= 1,NP
      A(I,J)=0.
      DO 58 K=1,M
      R=Y(J)*CC(K)-X(I)*SS(K)
      NN=(R+RMAX+DR)/DR
      IF(NN.GE.NP) GO TO 60
      IF(NN.LT.1) GO TO 60
      LP1=NN+1
      LM1=NN-1
      IF(LP2.GT.NP) LP2=NP
      IF(LM1.LT.1) LM1=1
      P=(R-X(NN))/DR
      COF3=.1666666*(B(LP2,K)-B(LM1,K))-.5*(B(LP1,K)-B(NN,K))
      COF2=.5*(B(LP1,K)+B(LM1,K))-B(NN,K)
      COF1=-.1666666*B(LP2,K)+B(LP1,K)-.333333*B(LM1,K)-.5*B(NN,K)
      P2=P*P
```

```
C*****AMOUNT OF FILTERING DEPENDS ON FT2=FILTER*FILTER**********
   58 BD(K)=P*(P2+FT2)*COF3+(P2+.666666*FT2)*COF2+P*COF1+B(NN,K)
C     INTEGRATE OVER THETA USING TRAPEZOIDAL INTEGRATION*********
      VAL=0.0
      DO 59 L=2,M
   59 VAL=VAL+BD(L)+BD(L-1)
      A(I,J)=VAL*DEL/2.
C**************************************************************
   60 CONTINUE
   61 CONTINUE
C
C**************************************************************
C
      NPN=NP+NPL
      IF(MODE.LT.4) GO TO 63
      IF(MODE.EQ.4) MODE=5
      GO TO 19
   63 IF(MODE.LT.3) GO TO 65
C
C*****CHANGE REFRACTIVE INDEX FIELD TO DENSITY FIELD*************
C
      DO 64 I=1,NP
      DO 64 J=1,NP
   64 A(I,J)=RHOINF+.4443*XLAMD*A(I,J)
C
C**************************************************************
C
      WRITE(6,114)
      GO TO 66
   65 WRITE(6,115)
   66 WRITE(6,113)
C
C*****WRITE REFRACTIVE INDEX OR DENSITY FIELD********************
C
      K=1
      K21=21
   67 WRITE(6,106)
      WRITE(6,110) (X(I),I=K,K21)
      DO 68 I= 1,NP
      NN=NP-I+1
   68 WRITE(6,111) Y(NN),(A(J,NN),J=K,K21)
      IF(K21.EQ.NP) GO TO 69
      K=K21+1
      K21=K21+21
      IF(K21.GT.NP) K21=NP
      GO TO 67
```

```
C*************************************************************************
C
   69 WRITE(6,116)
C
C*****WRITE FRINGE SHIFT INFORMATION*************************************
C
      WRITE(6,104) (TH(K),K=1,NT)
      DO 70 I=N,NPN
   70 WRITE(6,105) RB(I),(BB(I,J),J=1,NT)
      WRITE(6,117)
      WRITE(6,104) (TH(K),K=1,M)
      DO 71 I=1,NP
   71 WRITE(6,105) X(I),(B(I,J),J=1,M)
C
C*************************************************************************
C
C
C*****PLOT DENSITY OR REFRACTIVE INDEX ALONG 0,45,-45,AND 90 DEGREES*****
C
      K=1
      IF(MODE.GT.2) K=3
      IT(9)=ITSUB(K)
      IT(10)=ITSUB(K+1)
      IT(11)=ITSUB(7)
      IT(12)=ITSUB(8)
C     PLOT DENSITY ALONG THETA = 0.0 DEGREES
      CALL DRAW(NP,X,A(1,N),0,0,LAB,IT,0,0,0,0,0,0,9,3,0,LAST)
      DO 72 I=1,NP
   72 A(I,N)=A(N,I)
      IT(11)=ITSUB(5)
      IT(12)=ITSUB(6)
C     PLOT DENSITY ALONG THETA =90.0 DEGREES
      CALL DRAW(NP,X,A(1,N),0,0,LAB,IT,0,0,0,0,0,0,9,3,0,LAST)
      DO 73 I=1,NP
      X(I)=1.414*X(I)
   73 A(I,N)=A(I,I)
      IT(11)=ITSUB(9)
      IT(12)=ITSUB(10)
C     PLOT DENSITY ALONG THETA =45.0 DEGREES
      CALL DRAW(NP,X,A(1,N),0,0,LAB,IT,0,0,0,0,0,0,9,3,0,LAST)
      DO 74 I=1,NP
      K=NP-I+1
   74 A(I,N)=A(K,I)
      IT(11)=ITSUB(11)
      IT(12)=ITSUB(12)
C     PLOT DENSITY ALONG THETA =-45.0 DEGREES
      CALL DRAW(NP,X,A(1,N),0,0,LAB,IT,0,0,0,0,0,0,9,3,0,LAST)
```

```
C     ***************************************************************
CC
   75 CONTINUE
      STOP
      END

      SUBROUTINE COEF(VAL,SLOPE,U,CU2,CU,CONST)
C     ***************************************************************
CCC   *                                                             *
CCC   *  SUBROUTINE COEF CALCULATES THE COEFICIENTS USED BY  THE    *
CCC   *  FUNCTION (F1) TO EXPAND THE FRINGE INFORMATION TO 2 RMAX   *
CCC   *                                                             *
C     ***************************************************************
      U2=U*U
      CU2=-SLOPE/U-VAL/U2
      CU=-VAL/U-3.*U*CU2
      CONST=VAL-CU*U-CU2*U2
      RETURN
      END

      SUBROUTINE INPUT(XI,YJ,VAL)
C     ***************************************************************
CC    *                                                             *
CCC   *  SUBROUTINE INPUT IS SUPPLIED BY THE USER FOR MODE 1        *
CCC   *  OPERATION.  THE MAIN PROGRAM PASSES THE POINT (XI,YJ) AND  *
CCC   *  'INPUT' SUPPLIES THE VALUE OF THE REFRACTIVE INDEX AT THAT *
CCC   *  POINT USING ANY ARITHMETIC OR LOGIC STATMENT NECESSARY.    *
CC    *                                                             *
C     ***************************************************************
      VAL=0.
C     VAL=F(XI,YJ)
      RETURN
      END
```

```
C     ***************************************************************
CC    *                                                             C
CC    *  THE INPUT DATA FILES USED IN THE TESTING ARE INCLUDED      *
CC    *                                                             C
CC    ***************************************************************
CC
C
C         THE AXISYMETRIC GAUSSIAN OF FIGURE 4

      SUBROUTINE INPUT(XI,YJ,VAL)
      R2=XI**2+YJ**2
      VAL=EXP(-R2)
      IF(R2.GT.3.61) VAL=0.0
      RETURN
      END
C     NECESSARY CONTROL CARDS
    0.0       0.0
VAN HOUTEN GAUSSIAN TEST FUNCTION USING 151
DATA POINTS
  1.176     .6941
          1       151         1        99     2.000       0.0
    0.0       0.0
C
CC
C         THE AXISYMETRIC  SHOCK OF FIGURE 5

      SUBROUTINE INPUT(XI,YJ,VAL)
      R2=XI**2+YJ**2
      VAL=-.5*R2+2.
      IF(R2.GT.2.25) VAL=0.
      RETURN
      END,
C  NECESSARY CONTROL CARDS
VAN HOUTEN AXISYMETRIC SHOCK 151 DATA POINTS
WITH FILTER=1
  1.176     .6941
          1       151         1        99     2.000       1.0
    0.0       0.0


C         THE ASYMETRIC TEST CASE OF FIGURE 8
```

```
      SUBROUTINE INPUT(XI,YJ,VAL)
      Y2=YJ*YJ
      X2=XI*XI
      VAL=(1.-Y2)*EXP(-2.*X2)
      R2=Y2+X2
      IF(R2.GT.1.5) VAL = 0.
      RETURN
      END
C  NECESSARY CONTROL CARDS
VAN HOUTEN  ASYMMETRIC TEST  GAUSSIAN ON (X)
SQUARE ON (Y)
  1.176     .6941
        1       101         6         1       2.0        .5
    07.5      22.5      37.5      52.5      67.5      82.5
C
C         ACTUAL DATA FROM THE AXISYMMETRIC FREE JET AT Z=.5
C
C      NECESSARY CONTROL CARDS
VAN HOUTEN  AXISYMETRIC FREE JET Z=.5 FILTER=1.
101 DATA POINTS
  1.176     .6941
    3         101             1        99     1.25      1.0
     0.0      1.0
    0.00      0.00      0.03      0.32      0.82      1.33      1.93      2.19
    2.30      2.44      2.53      2.63      2.72      2.79      2.88      3.00
    3.15      3.36      3.60      3.80      4.00      4.28      4.64      4.94
    5.20      5.53      5.90      6.18      6.44      6.70      6.95      7.19
    7.40      7.61      7.80      7.97      8.12      8.22      8.48      8.62
    8.75      8.88      8.98      9.10      9.19      9.28      9.37      9.42
    9.44      9.46      9.48
C
C         ACTUAL DATA FROM THE TILTED FREE JET ASYMMETRIC CASE 61 POINTS
C
C  NECESSARY CONTROL CARDS
VAN HOUTEN 1913 0725  TILTED FREE JET
61 PTS  SYM=1
  1.176     .6941
        3        61         9         1      1.50      1.0
     5.0       0.0
    0.00      0.00      0.00      0.00      0.00      0.10      0.50      1.45
    2.03      2.09      2.10      2.30      2.65      3.19      3.70      4.33
    4.90      5.39      5.89      6.35      6.88      7.20      7.62      8.04
    8.38      8.60      8.75      8.88      8.92      8.97      8.95      8.94
    8.89      8.78      8.69      8.30      7.96      7.60      7.15      6.63
    6.10      5.53      5.08      4.50      3.93      3.38      3.00      2.89
    2.75      2.62      2.18      1.78      1.16      0.40      0.06      0.00
    0.00      0.00      0.00      0.00      0.00         .         .         .
    15.0      0.0
```

0.00	0.00	0.00	0.00	0.00	0.00	0.00
2.12	0.00	0.00	0.00	0.00	0.00	0.00
4.21	2.25	2.86	3.00	3.03	3.00	3.00
8.32	8.85	8.93	9.10	9.30	9.40	9.40
9.32	9.01	8.45	8.76	8.45	8.17	7.86
7.14	6.12	5.02	5.50	5.02	4.53	4.02
3.00	2.63	2.00	2.43	2.00	1.38	0.80
0	0	0	0	0	0	0
0.00	0.00	0.00	0.00	0.00	0.00	0.00
2.50	0.00	0.00	0.00	0.00	0.00	0.00
3.08	2.64	2.86	2.71	3.00	3.02	3.50
7.11	7.18	7.95	7.80	7.87	7.62	7.44
8.60	8.22	7.87	8.30	8.72	8.17	9.40
3.00	6.27	4.04	5.30	4.04	1.64	7.86
0	2.00	2.00	2.00	2.00	1.38	4.02
3.50	0.00	0.00	0.00	0.00	0.00	0.80
0.00	0.00	0.00	0.00	0.00	0.00	0.00
2.37	2.66	2.78	2.96	3.11	3.28	3.44
4.10	4.62	5.22	5.77	6.28	6.70	7.14
7.08	8.00	8.89	8.72	8.93	9.05	9.08
9.12	9.66	9.78	8.75	8.50	8.24	7.95
7.30	6.10	6.12	5.66	5.12	4.62	4.10
3.00	3.00	2.86	2.66	2.34	1.87	1.00
0.45	0.00	0.00	0.00	0.00	0.00	0.00
0.00	0.00	0.00	0.00	0.00	0.00	0.00
2.23	2.51	2.60	2.63	2.77	2.40	1.10
4.62	5.47	6.01	6.57	7.10	7.66	8.03
8.67	8.89	9.13	9.33	9.53	9.69	9.71
9.73	9.65	9.50	9.22	8.90	8.52	8.15
7.89	8.88	9.32	8.80	8.13	8.30	7.77
2.00	6.50	6.10	5.65	5.12	4.30	3.00
0.55	2.00	2.00	1.60	1.00	0.28	0.00
0.00	0.00	0.00	0.00	0.00	0.00	0.00
0.00	0.00	0.00	0.00	0.00	0.00	0.00
2.51	2.72	2.78	2.96	3.11	3.28	3.44
5.24	6.22	6.22	5.77	6.28	6.70	7.14
8.63	9.20	8.50	8.72	8.93	9.05	9.08
9.57	9.66	8.89	8.75	8.50	8.24	7.95
7.11	6.10	6.12	5.66	5.12	4.62	4.10
2.00	3.00	2.86	2.66	2.34	1.87	1.00
0.00	0.00	0.00	0.00	0.00	0.00	0.00
0.00	0.00	0.00	0.00	0.00	0.00	0.00
0.58	0.00	0.00	0.00	0.00	0.00	0.00
2.05	2.55	2.78	2.59	2.78	3.05	3.45
5.05	5.56	6.62	6.11	6.62	7.10	7.55

8.32	0.000	0.022	2.93	7.45	8.68	7.00
9.69	2.402	2.993	7.45	8.68	7.00	2.62
8.007	4.32	3.45	8.68	7.00	2.62	0.00
3.307	7.709	7.45	8.68	7.00	2.62	
0.75.0	9.198	8.68	7.00	2.62	0.00	
	7.388	7.00	2.62	0.00		
	2.87	2.62	0.00			
	0.85.0	0.00				

8.62	0.000	0.008	2.38	4.42	7.77	8.60
9.65	2.308	2.382	4.42	7.77	8.60	6.64
7.58	4.782	4.422	7.77	8.60	6.64	2.25
2.94	8.020	7.772	8.60	6.64	2.25	0.00
0.00	9.102	8.602	6.64	2.25	0.00	
0.0	6.923	6.642	2.25	0.00		
	2.533	2.250	0.00			
	0.000	0.000				

9.00	0.000	0.038	2.38	5.08	8.50	6.20
9.53	2.300	2.381	5.08	8.50	6.20	2.00
7.17	5.352	5.088	8.50	6.20	2.00	0.00
2.53	8.355	8.508	6.20	2.00	0.00	
0.00	9.005	8.502	2.00	0.00		
	6.455	6.202	0.00			
	2.188	2.020				
	0.000	0.000				

9.28	0.002	0.036	2.30	5.56	8.32	8.35
9.34	2.422	2.306	5.56	8.32	8.35	5.70
6.59	5.822	5.566	8.32	8.35	5.70	1.70
2.12	8.862	8.325	8.35	5.70	1.70	0.00
0.00	8.965	8.350	5.70	1.70	0.00	
	5.426	5.700	1.70	0.00		
	1.699	1.700	0.00			
	0.000	0.000				

9.50	0.507	0.808	2.39	5.95	8.50	8.20
9.10	2.672	2.395	5.95	8.50	8.20	5.12
5.80	6.290	5.958	8.50	8.20	5.12	1.17
1.50	8.865	8.508	8.20	5.12	1.17	0.00
0.00	5.426	8.202	5.12	1.17	0.00	
	1.066	5.120	1.17	0.00		
	0.000	1.170	0.00			
		0.000				

9.62	1.207	1.254	2.70	6.35	8.62	7.98
8.90	2.978	2.707	6.35	8.62	7.98	4.52
5.17	6.909	6.358	8.62	7.98	4.52	0.47
0.84	8.842	8.628	7.98	4.52	0.47	
0.	4.788	7.988	4.52	0.47		
	0.388	4.525	0.47			
	0.	0.477				

9.66	1.844	1.612	3.72	6.68	8.70	7.70
8.70	3.388	3.726	6.68	8.70	7.70	3.89
4.54	7.000	6.688	8.70	7.70	3.89	0.09
0.10	9.107	8.707	7.70	3.89	0.09	
0.	8.417	7.708	3.89	0.09		
	0.000	3.898	0.09			
	0.	0.097				

9.69	2.288	1.920	3.50	7.03	8.70	7.38
8.38	3.382	3.503	7.03	8.70	7.38	3.25
3.90	7.381	7.030	8.70	7.38	3.25	0.00
0.00	9.215	8.707	7.38	3.25	0.00	
0.	7.405	7.388	3.25	0.00		
	3.400	3.258	0.00			
	0.000	0.000				

LIST OF REFERENCES

1. Matulka, R. D., The Application of Holographic Interferometry to the Determination of Asymmetric Three-Dimensional Density Fields in Free-jet Flow, Ph.D. Thesis, Naval Postgraduate School, June, 1970.

2. Collier, R. J., Burckhardt, C.B., and Lin, L.H., Optical Holography, pp. 81-95, 311-365, Academic Press, 1971.

3. Jagota, R.C. and Collins, D.J., "Finite Fringe Holographic Interferometry Applied to a Right Circular Cone at Angle of Attack," to be published in Journal of Applied Mechanics.

4. Rowley, P.D., "Quantitative Interpretation of Three-Dimensional Weakly Refractive Phase Objects Using Holographic Interferometry," Optical Society of America, v. 59, pp. 1496-1498, 8 November 1969.

5. Junginger, H.G. and Van Haeringer, W., "Calculation of Three-Dimensional Refractive-Index Field Using Phase Integrals," to be published in Optics Communications.

6. Sweeney, D.W. and Vest C. M., "Reconstruction of Three-Dimensional Refractive Index Fields by Holographic Interferometry," Applied Optics, v. 11, pp. 205-207, 7 January 1972.

7. Matulka, R.D. and Collins, D.J., "Determination of Three-Dimensional Density Fields From Holographic Interferometry," Journal of Applied Physics, v. 42, pp. 1109-1119, 1 March 1971.

8. Craig, E.G., Laplace and Fourier Transforms for Electrical Engineers, pp. 332-379, Holt, Rinehart, and Winston, Inc., 1964.

9. Fowles, G.R., Introduction to Modern Optics, pp. 144-146, Holt, Rinehart, and Winston, Inc., 1968.

10. Froberg, Carl-Erik., Introduction to Numerical Analysis, pp. 195-223, Addison-Wesley Publishing Company, 1965.

INITIAL DISTRIBUTION LIST

		No. Copies
1.	Defense Documentation Center Cameron Station Alexandria, Virginia 22314	2
2.	Library, Code 0212 Naval Postgraduate School Monterey, California 93940	2
3.	Chairman, Department of Aeronautics, Code 57Be Naval Postgraduate School Monterey, California 93940	1
4.	Professor D. J. Collins, Code 57Co Department of Aeronautics Naval Postgraduate School Monterey, California 93940	3
5.	Lt Paul E. Van Houten, USN USS America CVA-66 c/o FPO New York, New York 09501	1

Security Classification

DOCUMENT CONTROL DATA - R & D

(Security classification of title, body of abstract and indexing annotation must be entered when the overall report is classified)

ORIGINATING ACTIVITY (Corporate author)

Naval Postgraduate School
Monterey, California

2a. REPORT SECURITY CLASSIFICATION

Unclassified

2b. GROUP

REPORT TITLE

The Application of Holographic Interferometry to the Determination of Discontinuous Three-Dimensional Density Fields

DESCRIPTIVE NOTES (Type of report and inclusive dates)

Engineer's Thesis; December 1972

AUTHOR(S) (First name, middle initial, last name)

Paul Edgar Van Houten

REPORT DATE	7a. TOTAL NO. OF PAGES	7b. NO. OF REFS
December 1972	69	10

8a. CONTRACT OR GRANT NO.	9a. ORIGINATOR'S REPORT NUMBER(S)
b. PROJECT NO.	
c.	9b. OTHER REPORT NO(S) (Any other numbers that may be assigned this report)
d.	

10. DISTRIBUTION STATEMENT

Approved for public release; distribution unlimited.

11. SUPPLEMENTARY NOTES	12. SPONSORING MILITARY ACTIVITY
	Naval Postgraduate School Monterey, California 93940

13. ABSTRACT

A fourier transform method is used to invert the integral equation resulting from holographic interferometry of three-dimensional weakly refractive phase objects. The inverted equation is applied to the determination of aerodynamic density fields. The effects of various numerical techniques are extensively evaluated in an attempt to minimize computational effort. Numerical filtering techniques are introduced in order to handle the discontinuities associated with supersonic aerodynamic phenomenon.

DD FORM 1 NOV 68 1473 (PAGE 1)

S/N 0101-807-6811

Security Classification

A-31408

14. KEY WORDS	LINK A		LINK B		LINK C	
	ROLE	WT	ROLE	WT	ROLE	WT
holographic interferometry						

Thesis
V168 Van Houten
c.1 The application of holographic interferometry to the determination of discontinuous three-dimensional density fields.